Complex Dynamics and Statistics in Hamiltonian 1-D Lattices

Tassos Bountis

Department of Mathematics, School of Science and Technology, Nazarbayev University

Astana, Republic of Kazakhstan

With the collaboration of:

Haris Skokos, currently Associate Professor of Mathematics at Cape Town University, South Africa

and my former Ph.D. students:

1) **L. Drossos**, currently Professor, Technol. Educational University of Western Greece, Mesolonghi

2) **Jeroen Bergamin**, currently school teacher at a Prototype High School in Amsterdam

3) **Christos Antonopoulos**, currently Lecturer of Mathematics at University of Essex, UK

4) **Thanos Manos**, currently researcher at Institute of Neuroscience and Medicine at Julich, Germany

5) **Eleni Christodoulidi**, currently Post-doctoral Fellow with Ch. Efthymiopoulos at Research Center of Astronomy and Applied Mathematics, Academy of Athens

Outline of the Lecture

1. Introductory remarks

2. Simple Periodic Orbits, Weak and Strong Chaos

3. Dynamical Indicators of Order and Chaos

4. Localization on 1-Dimensional Lattices

5. Thermostatistics of Chaotic Hamiltonian Systems

6. The Role of Long Range Interactions

This lecture is based on my book (co-authored with Haris Skokos) "Complex Hamiltonian Dynamics" (Springer Synergetic Series, April 2012).

1. INTRODUCTION

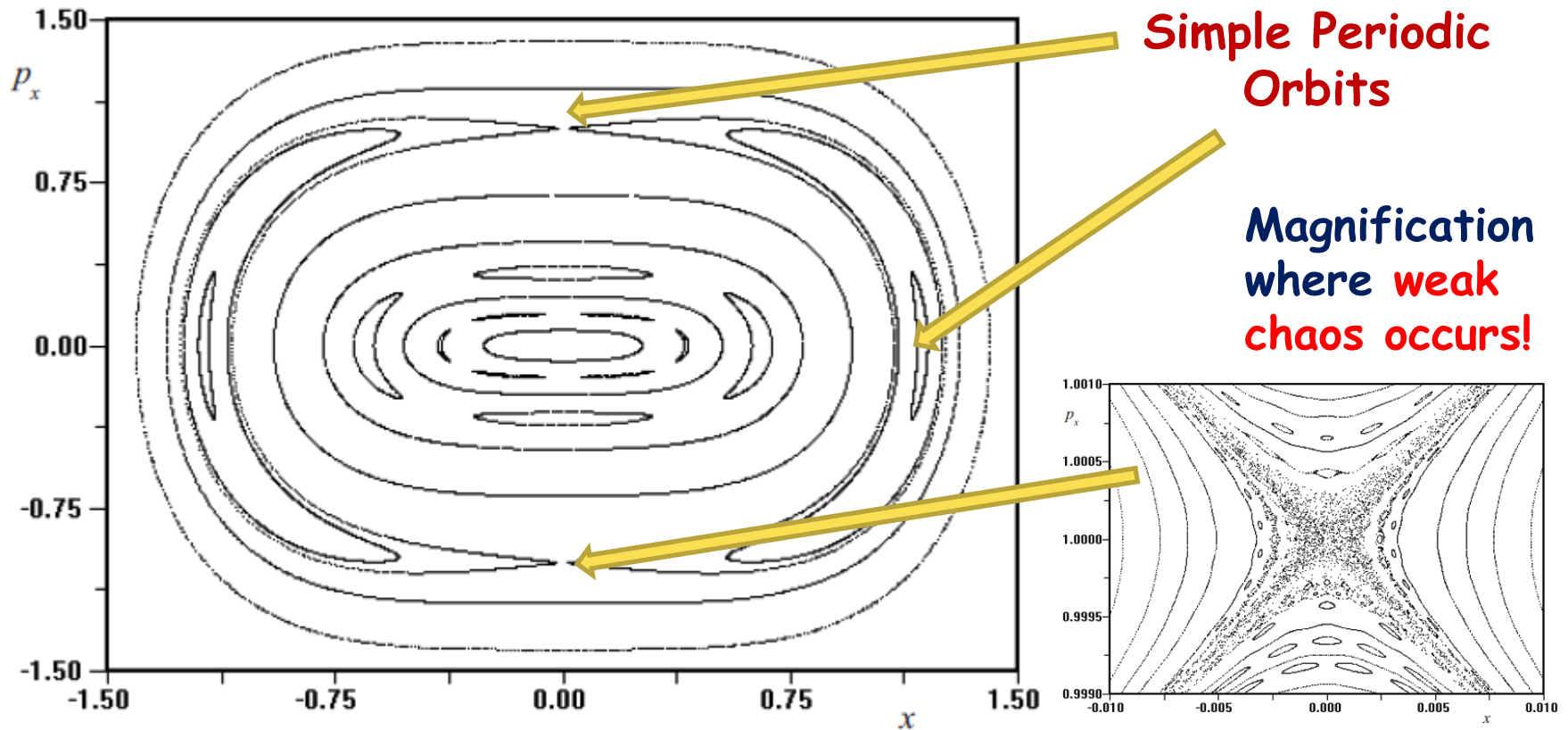$$H = H_0 + \varepsilon H_1 = \frac{1}{2}\left(p_x^2 + p_y^2\right) + \frac{1}{4}\left(x^4 + y^4\right) + \varepsilon x^2 y^2$$

H=E, energy constant

The solution of the equations **for ε= 0 (the uncoupled case) leads to** the figure on the right, which is a surface of section plot on the plane $x(t_k)$, $p_x(t_k)$, (every time $y(t_k)=0$).
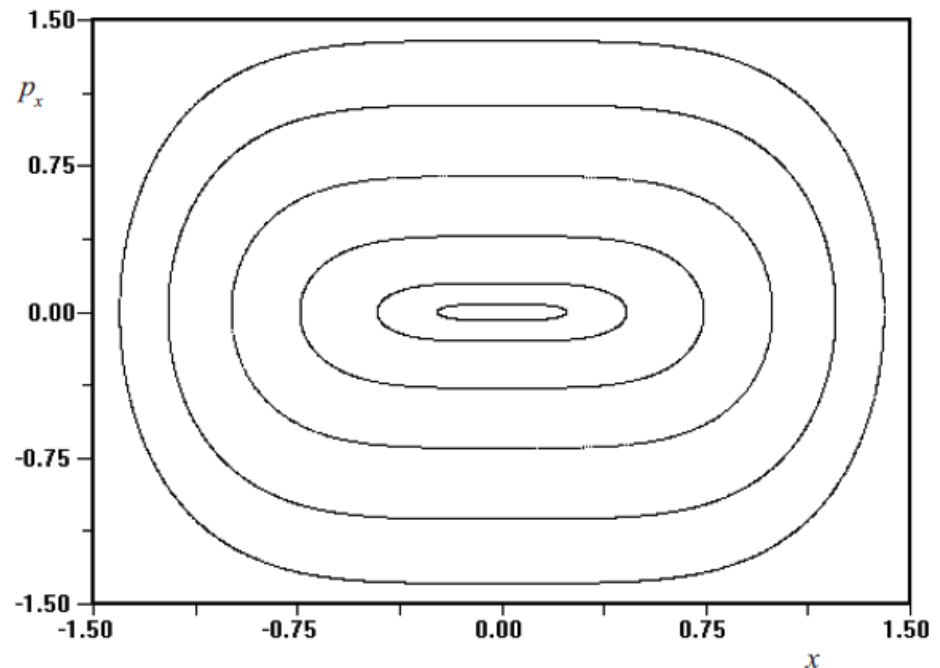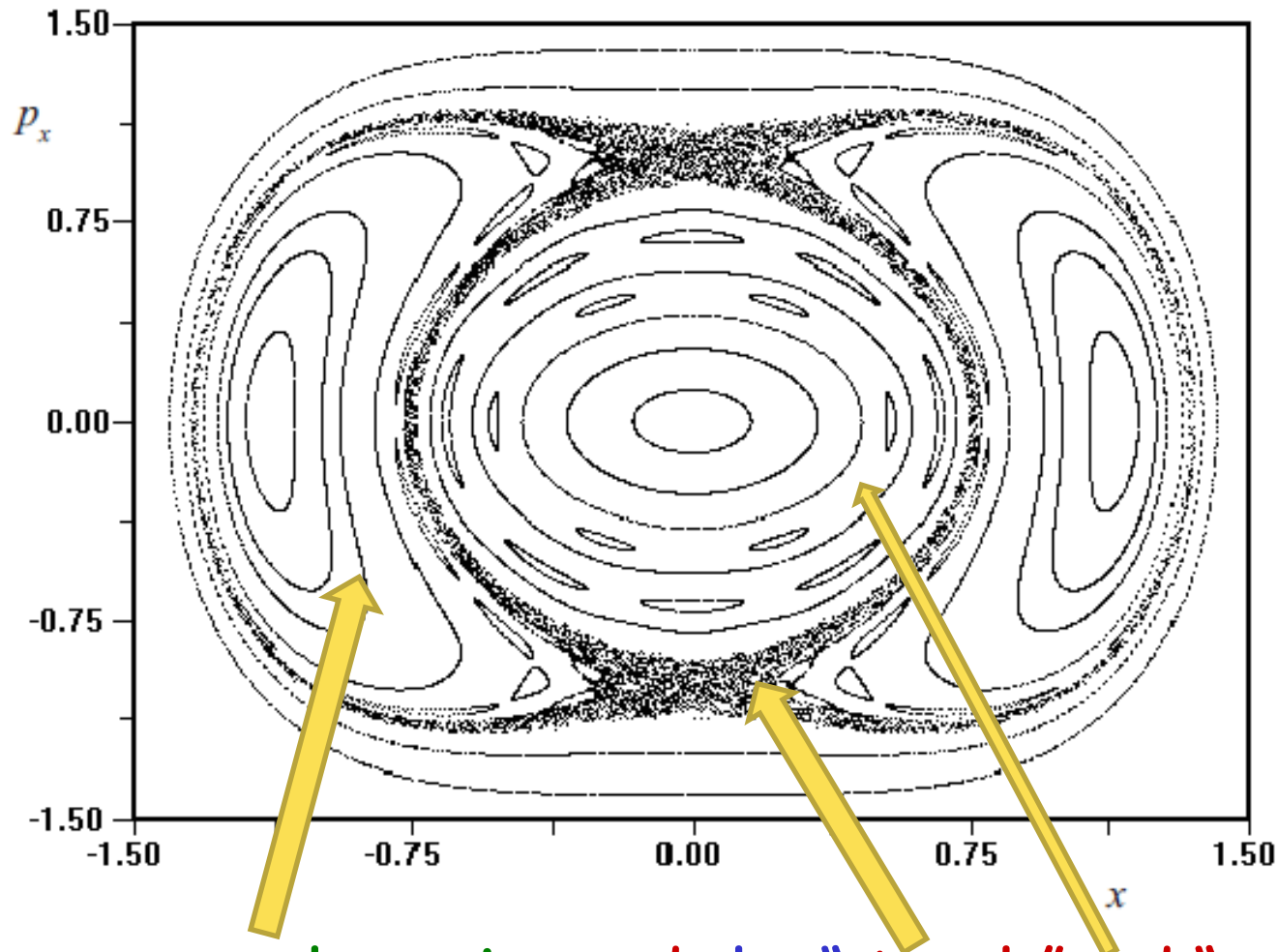

Thus, in the uncoupled (integrable) case, all curves correspond to periodic and quasiperiodic orbits with two frequencies w_1 and w_2.

How does chaos arise, when the coupling is turned on?

All we need to do is increase slowly the value of $\varepsilon > 0$ to discover an amazingly complex network of chaotic domains. Where are they?

Simple Periodic Orbits

Magnification where weak chaos occurs!

Surface of section of the orbits in the plane $x(t_k)$, $p_x(t_k)$, for $\varepsilon=0.02$

What happens if we further increase ε, say, ε=0.2?

There are regular regions and also "strongly" and "weakly" chaotic domains and they grow with E !

2. SIMPLE PERIODIC ORBITS, WEAK AND STRONG CHAOS

We study **Hamiltonian dynamical systems of N degrees of freedom** (dof), in an 2N – dimensional phase space of position and momentum coordinates, whose equations of motion are written in the form

(1)
$$\frac{dq_k}{dt} = \frac{\partial H}{\partial p_k} \quad , \quad \frac{dp_k}{dt} = -\frac{\partial H}{\partial q_k} \quad , \quad k = 1, 2, ..., N$$

H being the Hamiltonian function. If *H* does not explicitly depend on the time *t*, **it represents a first integral**, whose value **gives the total energy of the system** *E*. I will assume that the Hamiltonian can be expanded in *power series as a sum of homogeneous polynomials* of degree m ≥2

(2)
$$H = H_2\left(q_1, ..., q_N, p_1, ..., p_N\right) + H_3\left(q_1, ..., q_N\right) + ... = E,$$

so that **the origin is a stable equilibrium point of the system.**

We now assume that $H_m = 0$ for all m > 2 and that the linear equations resulting from (1) and (2), yield a matrix, whose eigenvalues all occur in conjugate imaginary pairs, $\pm i w_q$, and thus provide the frequencies of the so-called normal mode oscillations of the linearized system.

$$H_2 = \sum_{q=1}^{N} E_q = E, \quad E_q = \frac{1}{2}\left(P_q^2 + \omega_q^2 Q_q^2\right), \quad q = 1, 2, ..., N$$

where P_q , Q_q are the normal mode coordinates. Then, according to a famous theorem by Lyapunov, if none of the ratios of these eigenvalues, w_j/w_k is rational, for any j, k = 1,2,…,N, j ≠ k, all linear normal modes continue to exist as periodic solutions of the nonlinear system.

If the frequencies for $H_m \neq 0$ are close to those of the linear modes they are examples of what we call simple periodic orbits (SPOs), where all variables oscillate with the same frequency.

- What is the importance of these SPOs also called nonlinear normal modes (NNMs)? Once we have established that they exist, what can we say about their stability under small perturbations of their initial conditions?

- How do these properties change as we vary the total energy? Do such changes affect only the motion in the immediate vicinity of the NNMs or can they also influence the dynamics of the system more globally?

- Introducing the spectrum of Lyapunov exponents, I will point out how its properties are connected to the emergence of strongly (large scale) chaotic behavior in the solutions.

- I shall also describe the method of the Generalized Alignment Indices $GALI_k$, k=1,2,…,2N, which efficiently identify domains of chaos and order in N dof Hamiltonian systems and $2N$-dimensional (2N-D) symplectic maps.

3. INDICATORS OF REGULAR AND CHAOTIC DYNAMICS

 An interesting question in Hamiltonian dynamics concerns the connection between the local (linear) stability properties of simple periodic solutions of Hamiltonian systems, with the more "global" dynamics. Let us examine this question using the one-dimensional lattice (or chain) of coupled oscillators called the Fermi Pasta Ulam β-model described by the N dof Hamiltonian

$$H = \frac{1}{2}\sum_{j=1}^{N} p_j^2 + \sum_{j=1}^{N}\frac{1}{2}(x_{j+1} - x_j)^2 + \frac{\beta}{4}\sum_{j=1}^{N}(x_{j+1} - x_j)^4 = E \qquad (3)$$

where x_j are the displacements of the particles from their equilibrium positions, and $p_j = dx_j/dt$ are the momenta, β is a positive real constant and E is the total energy.

Let us focus on a some examples of simple periodic solutions (SPOs), which have well-defined symmetries and are known in closed form, for example:

(I) the out of phase (pi-mode)

$$\hat{x}_j(t) = -\hat{x}_{j+1}(t) = \hat{x}(t), \quad j = 1, 2, .., N$$

with N even, under periodic boundary conditions

(II) the SPO1 mode, where every 2 particles one is stationary and those on its either side move out of phase,

(III) the SPO2 mode, where every 3 particles one is stationary and the two on either side move out of phase both under fixed boundary conditions (fbc)

Figure 1 : **Examples of SPOs that we have called the Out of Phase (or pi-) Mode (above), the SPO1 orbit (middle) and the SPO2 orbit (below).**

Applying Lyapunov's Theorem we can prove the existence of SPOs as continuations of the linear normal modes of the system, whose energies and frequencies are

$$E_q = \frac{1}{2}\left(P_q^2 + \omega_q^2 Q_q^2\right), \qquad \omega_q = 2\sin\left(\frac{\pi q}{2(N+1)}\right), \quad q = 1, 2, ..., N \quad \textbf{(4)}$$

Thus, our SPO1 and SPO2 orbits, as NNMs, are identified by the indices q = (N+1)/2 and q = 2(N+1)/3 respectively.

An analytical criterion for "weak" chaos:

The above NNMs first destabilize at energy densities
$E_c/N \sim 1/N^\alpha$, α=1,2, as N→∞.

In agreement with an analytical criterion by Flach and co-workers, $E_c/N \sim \pi^2/6\beta N^2$, we find that for α = 2 orbits (like SPO2) instability implies "weak" chaos and the breakup of FPU recurrences. On the other hand, if α = 1, for which the SPO1 mode destabilizes we find "stronger" chaos.

3.1 Lyapunov exponents and "strong" chaos

Chaotic behavior is usually studied by evaluating the spectrum of Lyapunov exponents, L_i, i=1,....2N, (LEs) $L_1 = L_{max} > L_2 > .... > L_{2N}$, defined as follows:

$$K_t^i = \frac{1}{t} \ln \frac{\| w_i(t) \|}{\| w_i(0) \|}, \quad i.e. \quad L_i = \lim_{t \to \infty} K_t^i \qquad i=1,2,....,N \qquad (5)$$

If L_{max} > 0, the orbit is chaotic, while if L_{max} = 0 the orbit is stable. In the thermodynamic limit, where $E \to \infty$ and $N \to \infty$ (with E/N fixed), the Lyapunov spectrum near unstable NNMs tends to a smooth curve, see Figure 2(a).

For our two orbits SPO1 and SPO2, at low energies when they are unstable, we find that their Lyapunov spectra are distinct see Figure 2(b,c). Raising the energy, the Lyapunov spectra converge to the same exponentially decreasing function $L_i(N) \sim exp(-\alpha i/N)$, ,i=1,2,...,N, thus providing evidence that the orbits explore the same chaotic region.
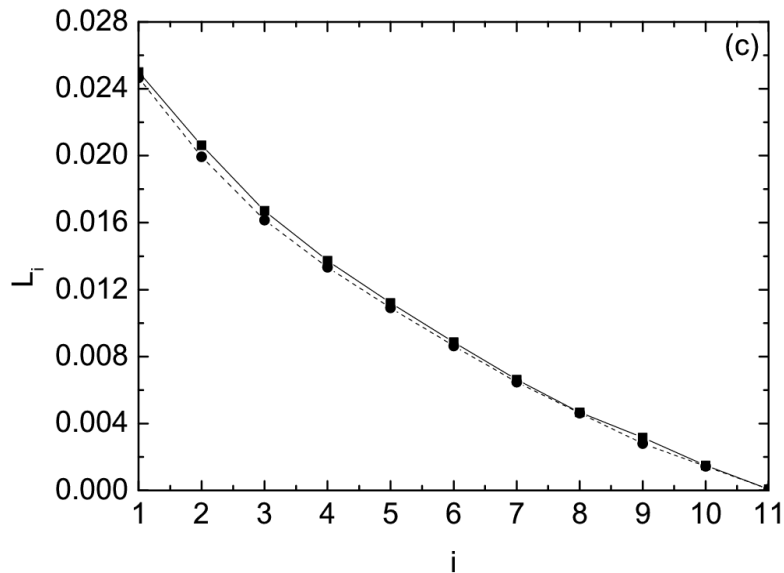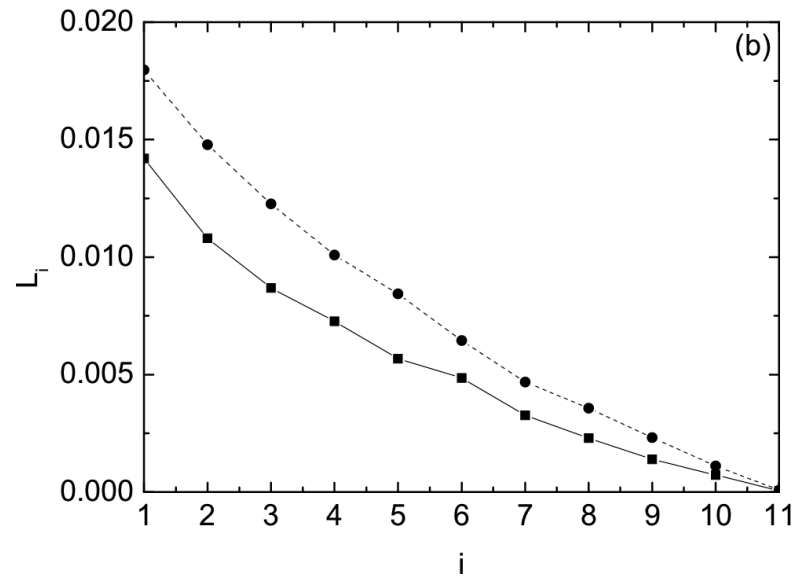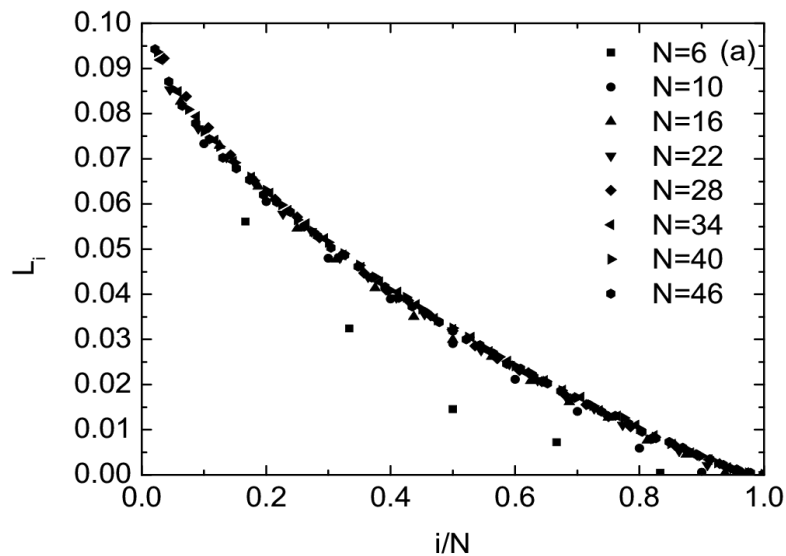
Figure 2. (a) The spectrum of Lyapunov exponents near an out of phase orbit of the β − FPU model as E and N grow (E/N=3/4). In (b) and (c) the Lyapunov spectra of solutions starting near unstable SPO1and SPO2 orbits converge, as the energy grows from E= 2.1 in (b) to E=2.6 for (c), indicating that the chaotic regions about these orbits have merged!

3.2 Beyond Lyapunov exponents: The Generalized Alignment Indices (GALI)

The GALI indicators: (a) detect the chaotic nature of the orbits more rapidly than other methods and, (b) identify quasiperiodic motion providing also the dimension of the torus.

The $GALI_k$, k = 2,...., N are defined, through the evolution of k initially linearly independent deviation vectors w_i (0), as the volume of a k-parallelepiped given by the wedge product

$$GALI_k = \| \hat{w}_1(t) \wedge \hat{w}_2(t) \cdots \wedge \hat{w}_k(t) \| \quad , \quad \text{i = 1,2,...,k} \qquad (6)$$

whose k edges are the unitary deviations $\hat{w}_i(t) = w_i(t)/\| w_i(t) \|$.

Thus, it is evident that if at least two of the deviation vectors become linearly dependent, the wedge product in (6) becomes zero and the $GALI_k$ vanishes.

Behavior of GALI$_2$ for chaotic motion

For chaotic orbits the two deviation vectors **tend to become linearly dependent** in the direction defined by the maximal Lyapunov exponent.

$\hat{w}_2(t)$

$\hat{w}_1(t)$

GALI$_2$ (t)

P(t)

$\hat{w}_2(0)$

$\hat{w}_1(0)$

GALI$_2$ (0)

P(0)
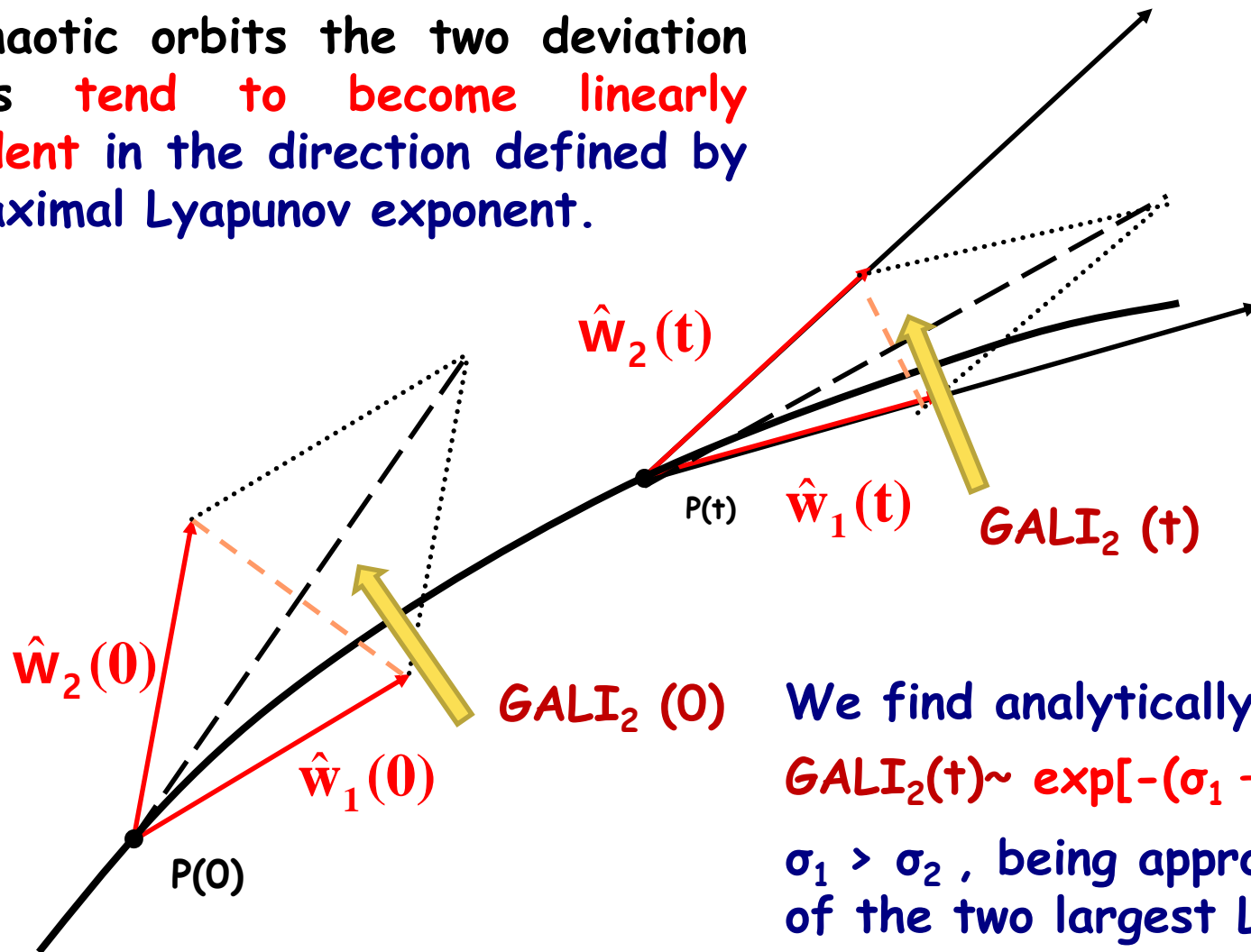
We find analytically:

GALI$_2$(t)~ exp[-($\sigma_1 - \sigma_2$)t]→0

$\sigma_1 > \sigma_2$, being approximations of the two largest Lyapunov exponents $L_1 > L_2$

Asymptotic analysis of the GALI$_2$ for chaotic motion

The evolution of a deviation vector can be approximated by :

$$\mathbf{v_1(t)} = \sum_{i=1}^{2n} \mathbf{c_i^{(1)} e^{\sigma_i t} \hat{e}_i} \approx \mathbf{c_1^{(1)} e^{\sigma_1 t} \hat{e}_1 + c_2^{(1)} e^{\sigma_2 t} \hat{e}_2} + \ldots$$

where $\sigma_1 > \sigma_2 > \ldots$ are the Lyapunov exponents.

Thus, we derive a leading order estimate for $\mathbf{v_1(t)}$:

$$\frac{\mathbf{v_1(t)}}{\|\mathbf{v_1(t)}\|} \approx \frac{\mathbf{c_1^{(1)} e^{\sigma_1 t} \hat{e}_1 + c_2^{(1)} e^{\sigma_2 t} \hat{e}_2}}{|\mathbf{c_1^{(1)}}| \mathbf{e^{\sigma_1 t}}} = \pm \hat{e}_1 + \frac{\mathbf{c_2^{(1)}}}{|\mathbf{c_1^{(1)}}|} \mathbf{e^{-(\sigma_1 - \sigma_2)t} \hat{e}_2}$$

and an analogous expression for $\mathbf{v_2(t)}$:

$$\frac{\mathbf{v_2(t)}}{\|\mathbf{v_2(t)}\|} \approx \frac{\mathbf{c_1^{(2)} e^{\sigma_1 t} \hat{e}_1 + c_2^{(2)} e^{\sigma_2 t} \hat{e}_2}}{|\mathbf{c_1^{(2)}}| \mathbf{e^{\sigma_1 t}}} = \pm \hat{e}_1 + \frac{\mathbf{c_2^{(2)}}}{|\mathbf{c_1^{(2)}}|} \mathbf{e^{-(\sigma_1 - \sigma_2)t} \hat{e}_2}$$

Now take their cross product:

$$GALI_2 = \| \hat{v}_1(t) \wedge \hat{v}_2(t) \| \approx \left\| \frac{c_2^{(1)}}{c_1^{(1)}} \pm \frac{c_2^{(2)}}{c_1^{(2)}} \right\| e^{-(\sigma_1 - \sigma_2)t}$$

Behavior of GALI$_2$ for regular motion

On a **torus of quasiperiodic motion** the two deviation vectors **become tangent to the torus,** since they are in general linearly independent between them.
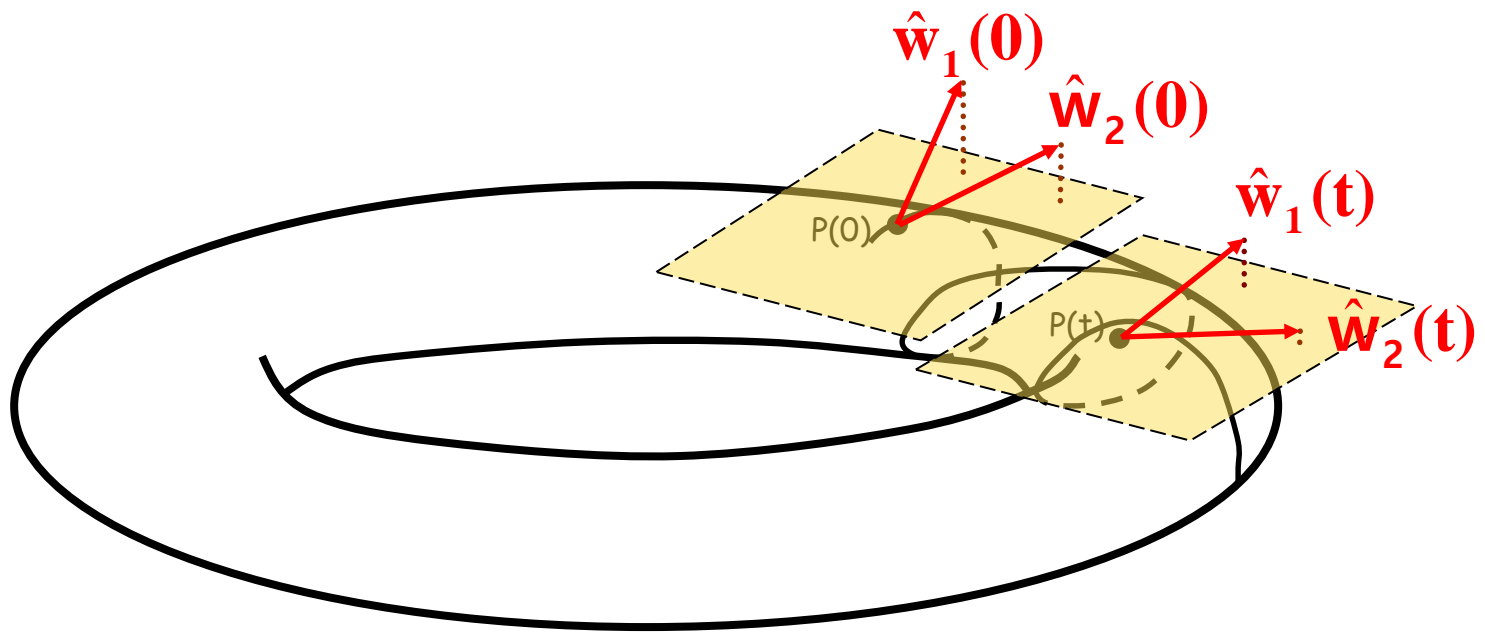
Hence for quasiperiodic motion, we find

GALI$_2$(t) ≈ const. for all t > 0

We have shown analytically that, for a chaotic orbit, all deviation vectors tend to align in the direction of L_1, and all GALI$_k$ tend to zero exponentially following the law

$$GALI_k \propto \exp\left(-\left(L_1 - L_2 + L_1 - L_3 + ... + L_1 - L_k\right)t\right), \quad t \to \infty \quad \text{(7)}$$

where L_i are the k largest LEs.

In the case of regular orbits lying on s-dimensional tori, all deviation vectors tend to fall on the tangent space of the torus. Thus, if we start with k ≤ s, the deviation vectors will remain linearly independent on the tangent space of the torus and the GALI$_k$ will be nearly constant, different from zero, for k ≤ s.

On the other hand, for k > s, all GALI$_k$ tend to zero as $t \to \infty$ following power laws, since some deviation vectors will eventually become linearly dependent.

$$GALI_k \propto \frac{1}{t^{k-s}} , \quad s < k \le 2N-s, \quad GALI_k \propto \frac{1}{t^{2(k-N)}} , \quad 2N-s < k \le 2N \quad \text{(8)}$$
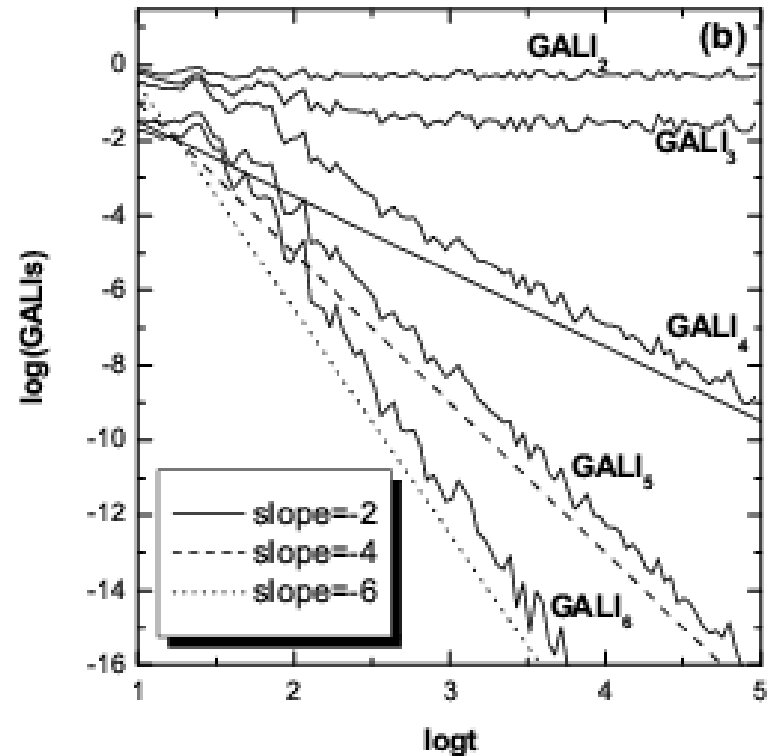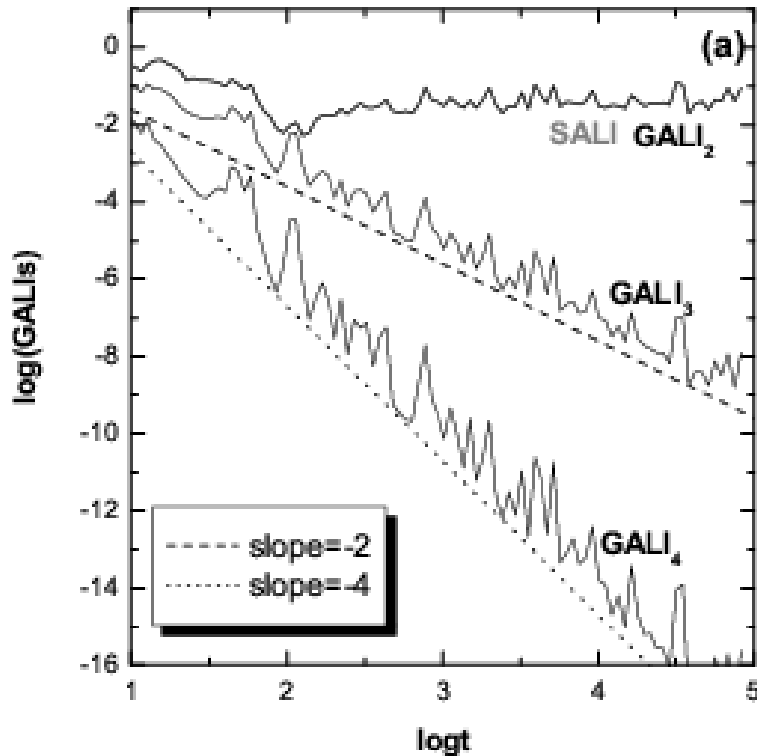
Figure 3. The GALI indices for a Hamiltonian system of (a) 2 degrees of freedom and (b) 3 degrees of freedom. In case (a), since only $GALI_2$ is constant the motion lies on a 2-dimensional torus, while in (b), where both $GALI_2$ and $GALI_3$ are constant, the torus is 3-dimensional.

4. LOCALIZATION IN 1-DIMENSIONAL LATTICES

4.1 Localization in Fourier space

In 1955, by E. Fermi, J. Pasta and S. Ulam (FPU) used the computers available at the Los Alamos National Laboratory to integrate a chain of 31 nonlinear oscillators, coupled to their nearest neighbors, and investigate how energy was shared by all normal modes of the system.

To their great surprise, starting with initial conditions placed on the $q = 1$ linear normal mode, they discovered, for small energies, a near-recurrence to their initial state after relatively short times exciting very few other modes, see Figure 4 (a).

This remarkable observation ran contrary to the expectation of energy sharing among all modes predicted by equilibrium statistical mechanics and was termed the "paradox" of FPU recurrences.
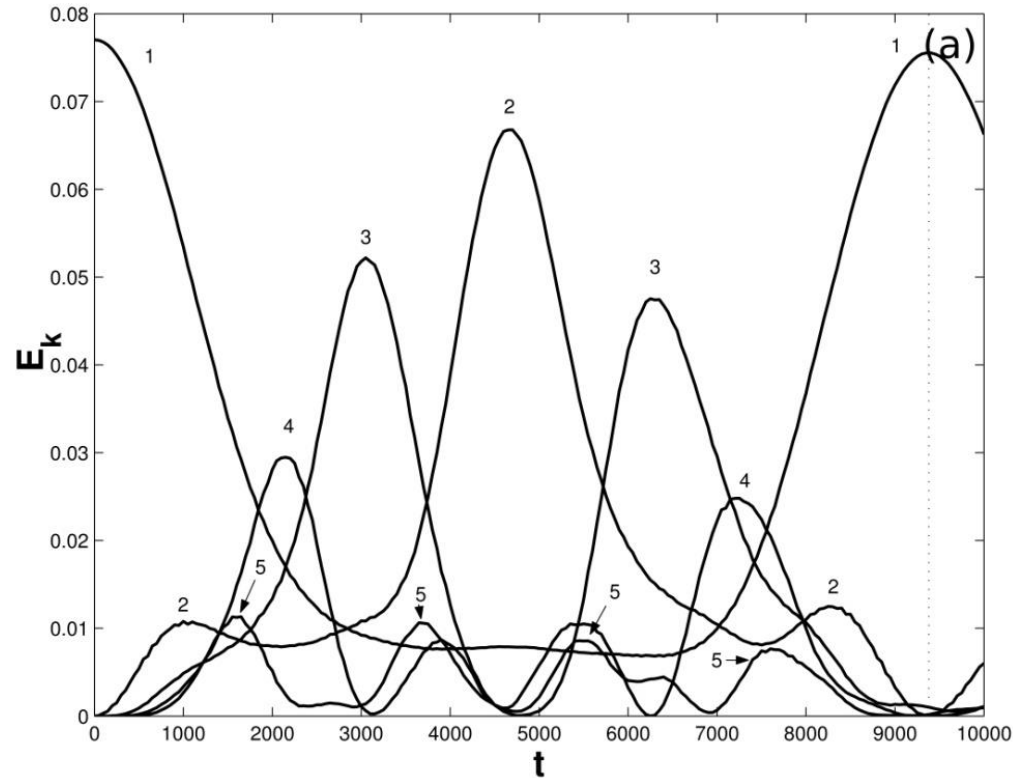
Figure 4: (a) **Localization in modal space** in the form of **FPU recurrences,** discovered by Fermi Pasta and Ulam, for a lattice of 31 particles. Note how only **a packet of about 5 modes** is excited before the energy returns to the $q = 1$ mode.

Energy localization" here implies localization in Fourier q-modal space, as the FPU recurrences were observed when all the energy was placed in the $q=1$ mode!

Flach and his co-workers in 2005 introduced the concept of q-breathers, as exact periodic solutions of the problem. They showed that if we excite a single low q-breather mode the total energy remains localized only within a few of these low frequency modes, also called metastable states or natural packets.

A more complete interpretation of the FPU paradox was provided by our group (Phys. Rev. E 81, 2010), where we introduced the concept of q-tori, reconciling q-breathers with the metastable packets of low-frequency modes.

Let us now use the GALI indices to study the stability of these q – tori and the breakdown of the associated FPU recurrences!
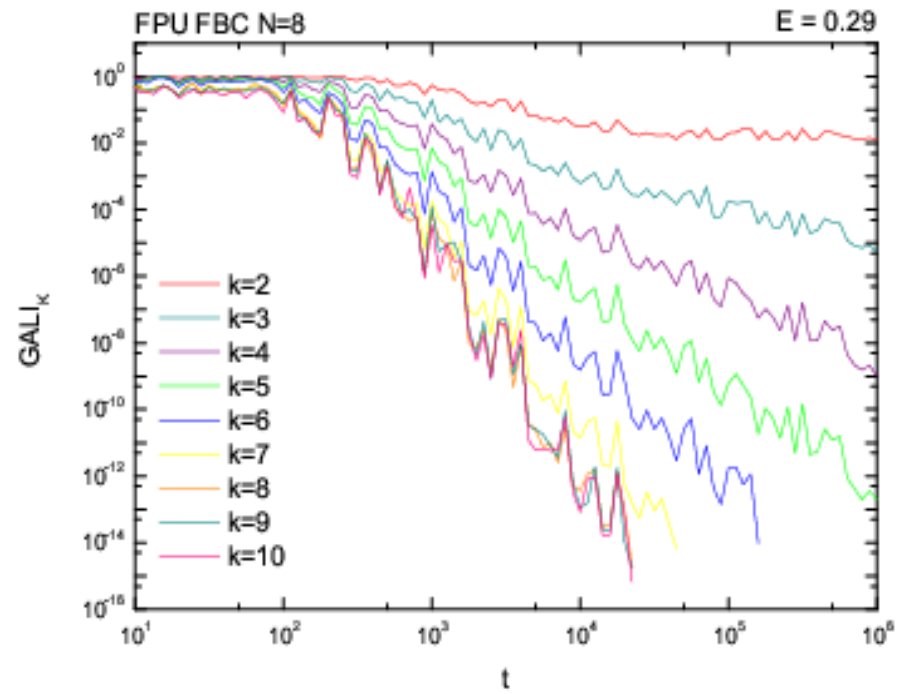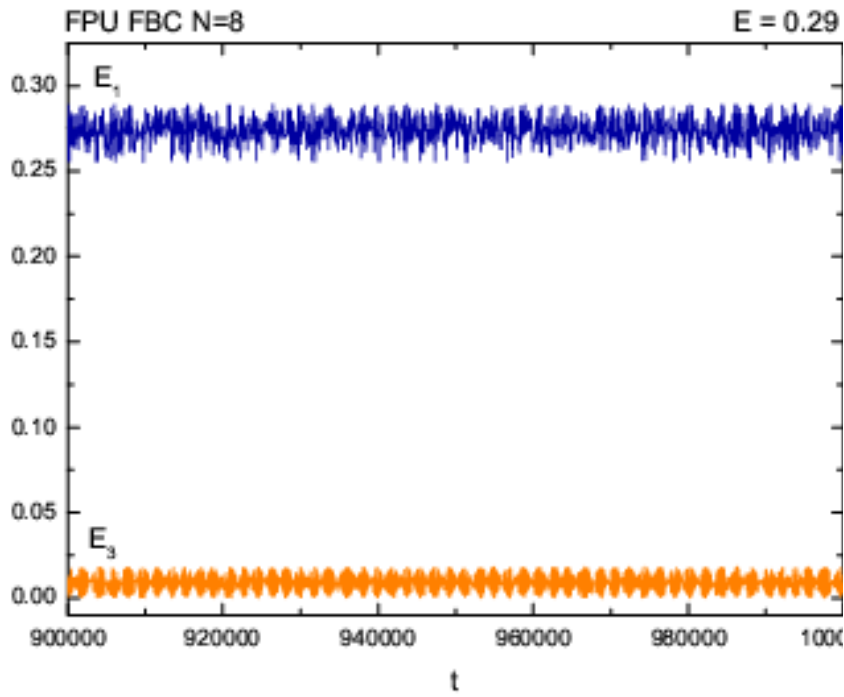
Figure 5: FPU with 8 particles: (a) Only the E_1 and E_3 modes are excited. Observe that the associated q-torus is 2-dimensional, since (b) only GALI$_2$ =const. and all other GALI$_k$ decay by power laws.
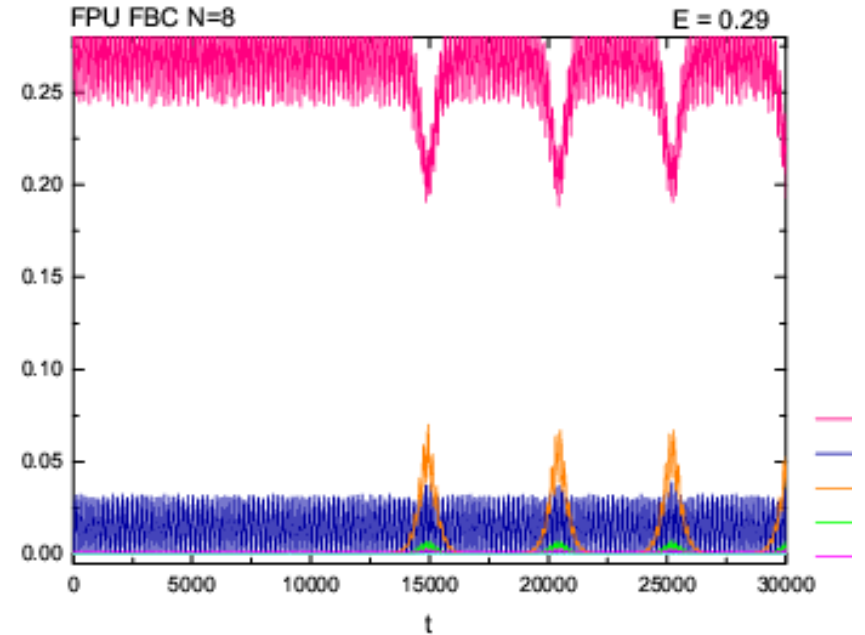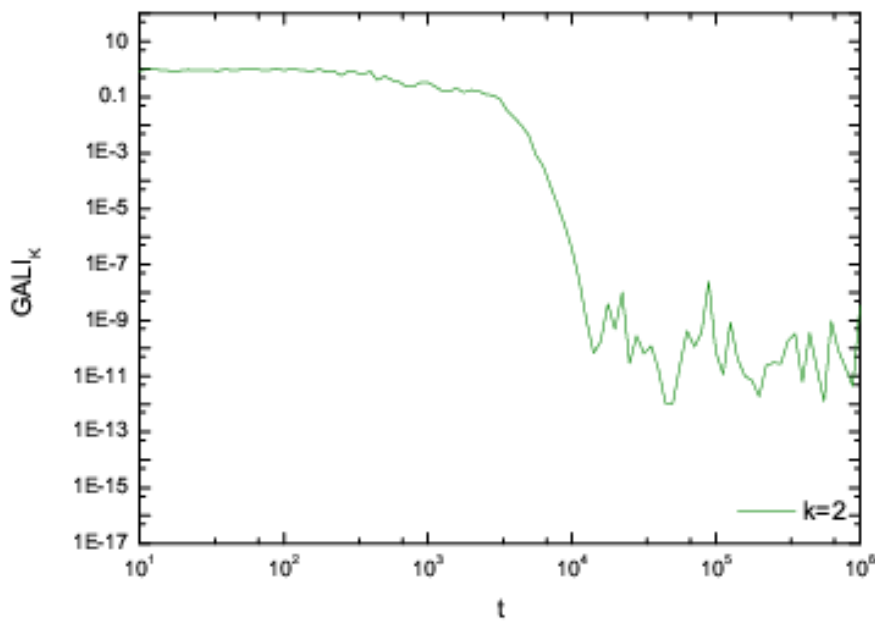
Figure 6: FPU with 8 particles and initial conditions near a q=2 torus: (a) The evolution of GALI$_2$ shows already at t ≈ 1000 that the orbit diffuses away from the torus weakly chaotically. (b) This becomes visible in the oscillations much later, when the recurrences break down at t ≈ 14000.

4.1 Localization in configuration space

It is also important to mention the localization of nonlinear lattices in their spatial coordinates. These are exponentially localized periodic oscillations, called discrete breathers. They have been verified analytically and numerically on a variety of lattices, like the Klein-Gordon (KG) chain

$$\ddot{x}_n = -V'(x_n) + \alpha(x_{n+1} - 2x_n + x_{n-1}), \quad V(x) = \frac{1}{2}Kx^2 + \frac{1}{4}x^4 \quad (9)$$

- $\infty < n < \infty$, where $V(x)$ is an on-site potential and $\alpha > 0$ is a coupling parameter. Expanding in Fourier series, one finds that discrete breathers are directly related to homoclinic orbits of invertible maps, through which one can prescribe a numerical procedure for constructing them to arbitrarily high accuracy.
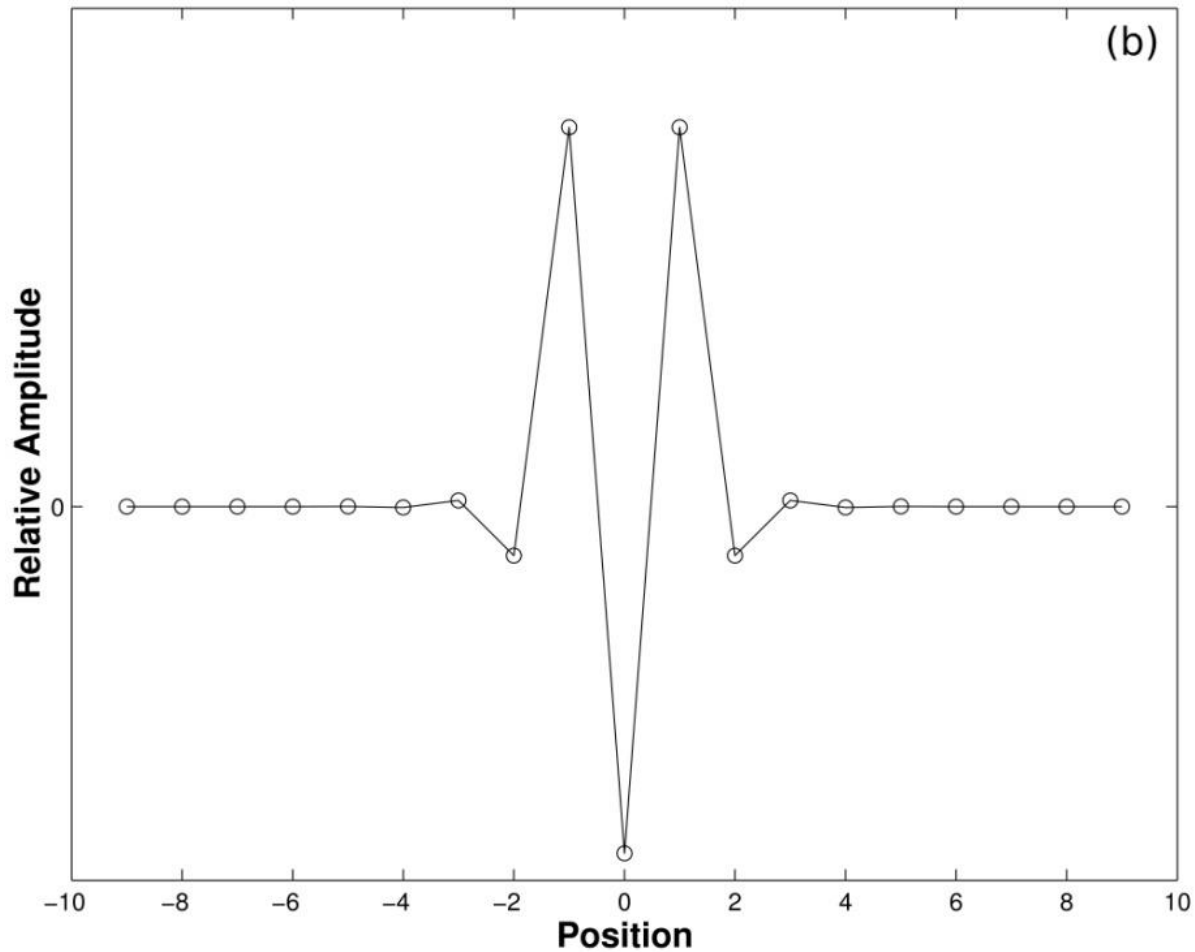
Figure 4(b) Localization in configuration space in the form of a discrete breather of a harmonic nearest neighbor chain with on site nonlinear potential of the Klein Gordon type.

Indeed, keeping only the leading term $x_n(t)=A_n\cos(\omega_b t)$ in such an expansion one obtains the map

$$A_{n+1} = -A_{n-1} + CA_n + \alpha^{-1}A_n^3 \quad , \quad C = -2 + (K - \omega_b^2)/\alpha \qquad (10)$$

which provides a very good approximation for the amplitudes A_n, as homoclinic orbits lying at the intersections of the invariant manifolds of the saddle point at the origin of (10), at $|C|>2$

Discrete breathers constitute one more example of what we call Simple Periodic Orbits, with all particles oscillating with frequency ω_b outside the phonon band of NNMs.

Does it happen that discrete breathers, when they are stable, are surrounded by low-dimensional tori? If so, it would be interesting to study the dimensionality of these tori and their stability using our GALI indices to determine if these localized solutions will eventually break down as time evolves!
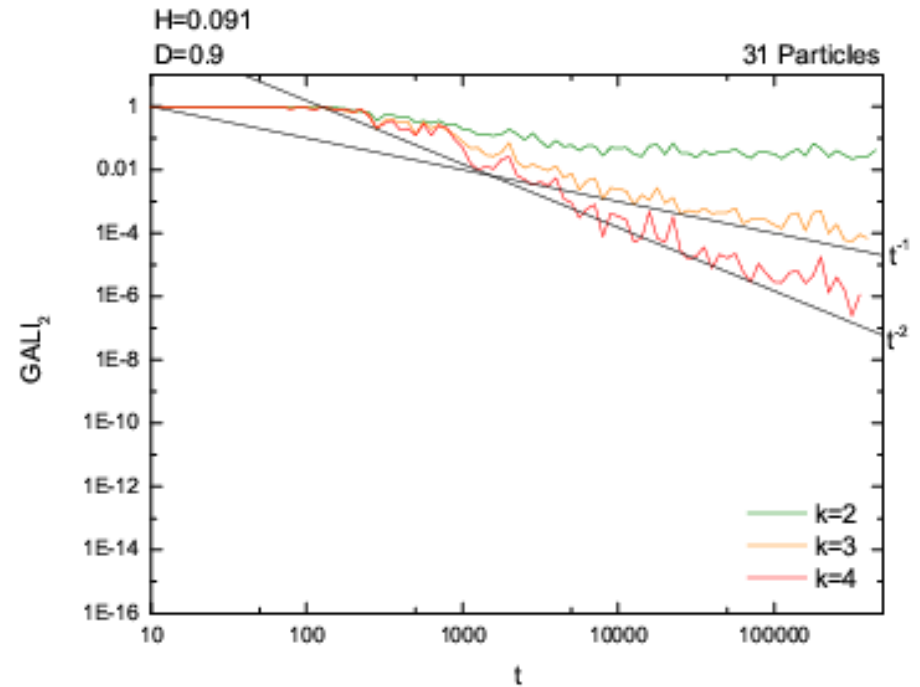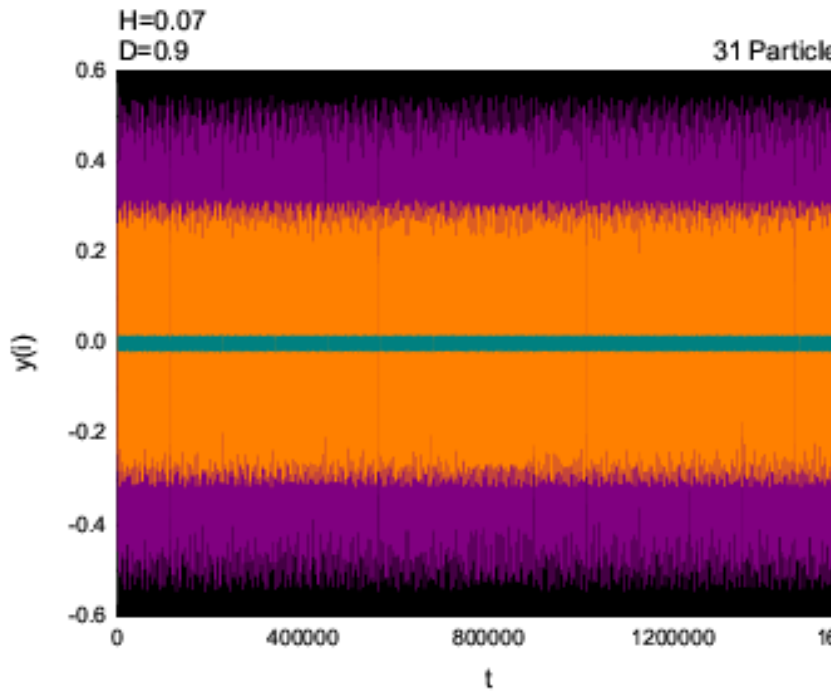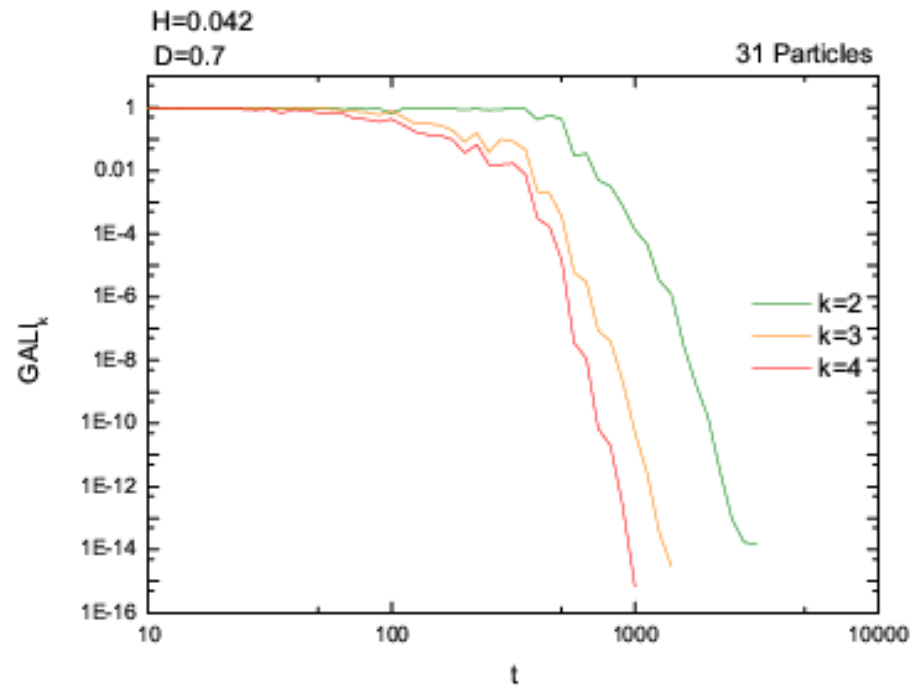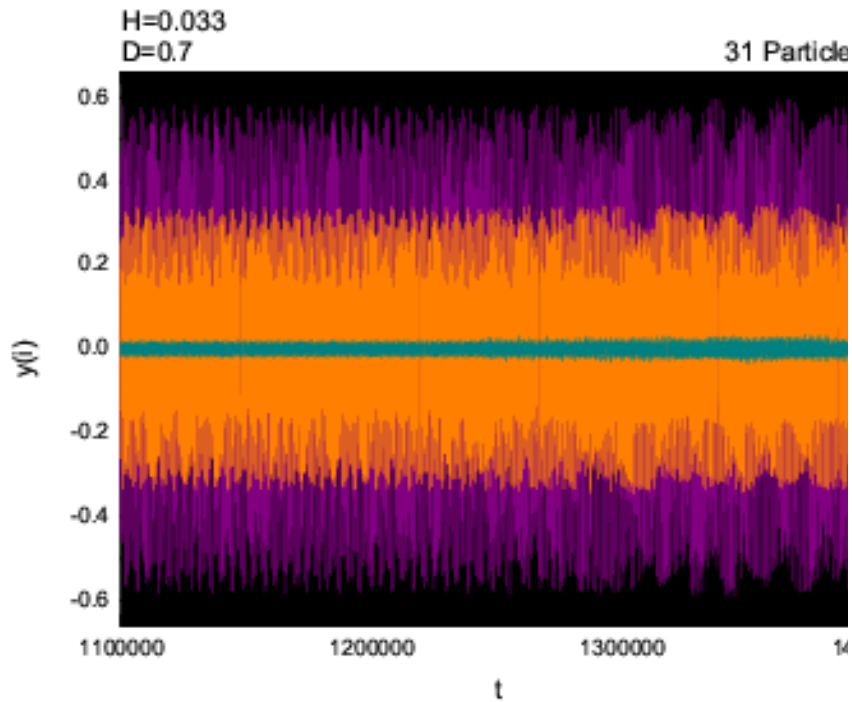
Figure 7 (STABLE TORUS): (a) The oscillations of the central three particles of a KG chain of N=31 particles do not break down, forming a quasiperiodic breather. (b) The torus is 2-dimensional, since only $GALI_2$ remains constant, while all other $GALI_k$ decrease by power laws.

Figure 8 (UNSTABLE TORUS):(a) The oscillations of the central 3 particles, starting further from the breather, appear quasiperiodic for very long times. (b) The solution, however, is chaotic and the "torus" eventually breaks down since the GALIs decay exponentially.

Here we can predict the torus breakdown after t ≈ 1000 (right), while it is observed after t ≈ 1400000 (left)!

5. COMPLEX STATISTICS OF CHAOTIC DYNAMICS

To study the statistical properties of chaotic behavior in Hamiltonian systems, we recall some basic facts of equilibrium thermodynamics. As is well-known, in Boltzmann - Gibbs statistics, if a system can be at any one of i=1,2,...,W states with probability p_i , its entropy is given by the famous formula

$$S_{BG} = -k \sum_{i=1}^{W} p_i ln \ p_i \ , \quad \text{under the constraint} \quad \sum_{i=1}^{W} p_i = 1 \quad \textbf{(11)}$$

where *k* is the Boltzmann's constant. The BG entropy satisfies the property of additivity, i.e. if *A* and *B* are two independent systems, their union entropy is $S_{BG}(A+B) = S_{BG}(A)+S_{BG}(B)$. At thermal equilibrium, and for a continuum set of states depending on one variable, *x*, the probability density that optimizes the BG entropy subject to the constraints (11), zero mean and variance *V* is, of course, the well-known Gaussian

$$p(x) = e^{-x^2/2V} \ / \ \sqrt{2V} \quad \textbf{(12)}$$

Another important property of the BG entropy is that it is *extensive*, i.e. that S_{BG}/N is finite in the limit $N \to \infty$. But, many physically important systems governed by long range interactions are neither additive nor extensive, like self-gravitating systems of finitely many mass points and ferromagnetic spin models. For such systems the so-called Tsallis entropy has been proposed (1988)

$$S_q = k \frac{1 - \sum_{i=1}^{W} p_i{}^q}{1-q} \quad , \quad \text{under the constraint} \quad \sum_{i=1}^{W} p_i = 1 \qquad (13)$$

depending on an index q. For a continuum set of states x, the Tsallis entropy is optimized by the q-Gaussian pdf

$$p_q(x) = a e_q^{-\beta x^2} = a \left(1 - (1-q)\beta x^2 \right)^{1/(1-q)} \qquad (14)$$

where $\beta = 1/kT$ is a free parameter and $a > 0$ a normalization constant. Expression (14) tends to a Gaussian, as $q \to 1$ $e_q \to e$. The Tsallis entropy is not additive, and, in general, non-extensive. It offers us the possibility of studying problems whose correlations decay by power laws (not exponentially).

## 5.1 The case of multi-degree-of freedom Hamiltonian systems

There are many situations in such systems where the dynamics is weakly chaotic and may, therefore, possess Tsallis statistics of the type described above.

We found that, in the β-FPU model, near an unstable SPO1 orbit of a 5-particle chain, orbits that remain "trapped" for very long times in a thin chaotic region (see Figures 9,10) are described by pdfs of the q-Gaussian type with $q \approx 2.8$, see Fig. 11(d).

These are what we call quasi-stationary states (QSS) of the dynamics. Following these states for long times, one typically finds that their pdfs pass through QSS described by q-Gaussians of smaller $q \approx 2.48$, see Fig. 11(e), until they finally converge to Gaussians with $q = 1$, when the orbits escape to a much larger domain of strong chaos, see Fig. 11(f).
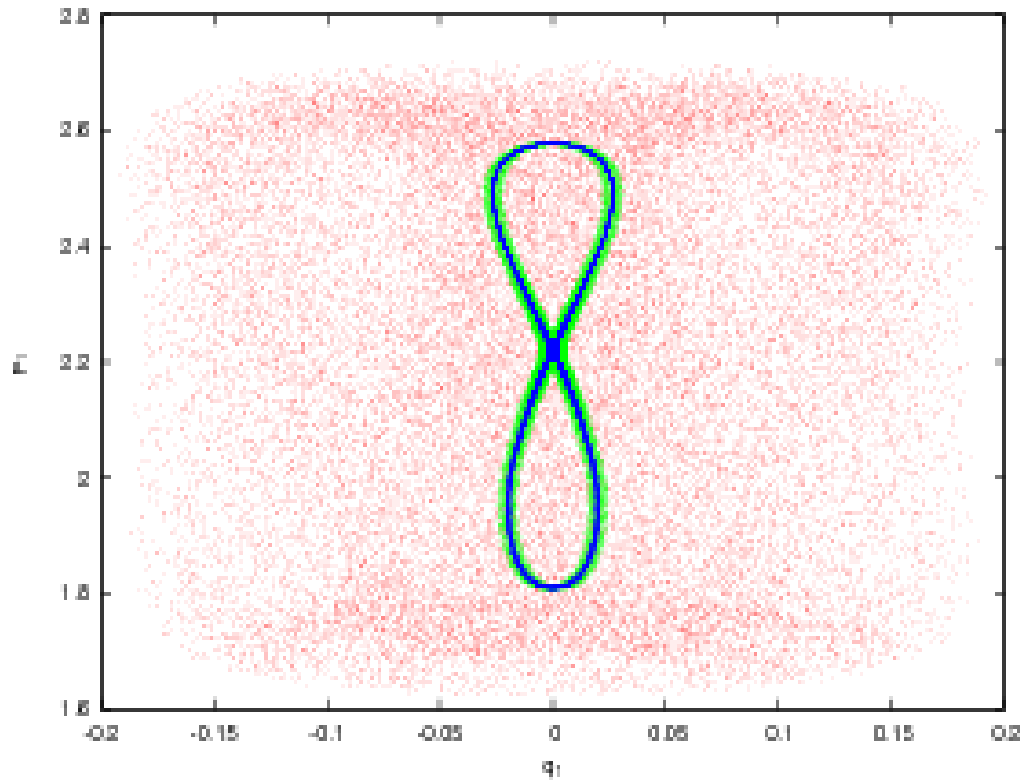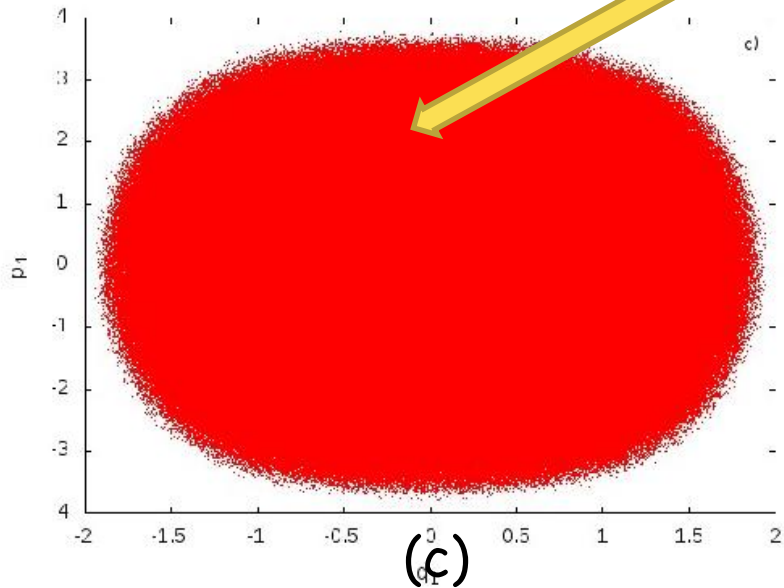
Figure 9: Three different orbits with initial conditions very close to an unstable SPO1 orbit of the 5 particle FPU-β chain: The black "figure eight" in the middle starts from a distance of 10^{-7} , the green one around it starts within 0.0001 and the red one extending over a much larger region, starts within 0.01 from the saddle point.
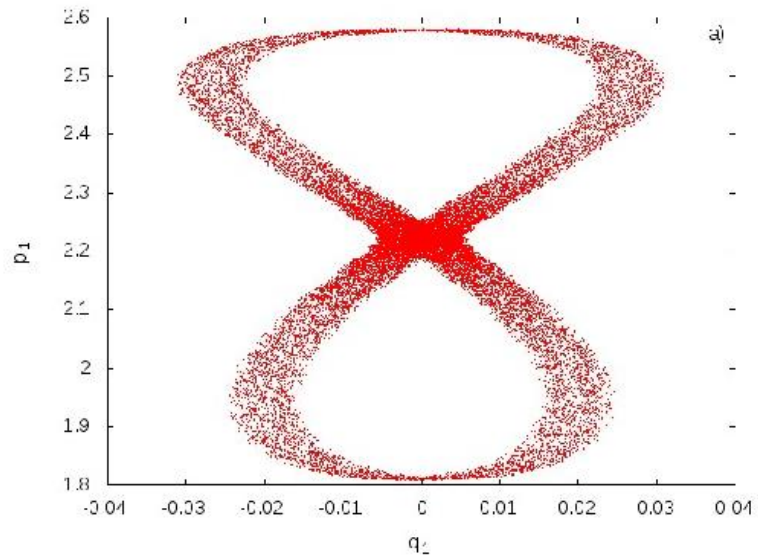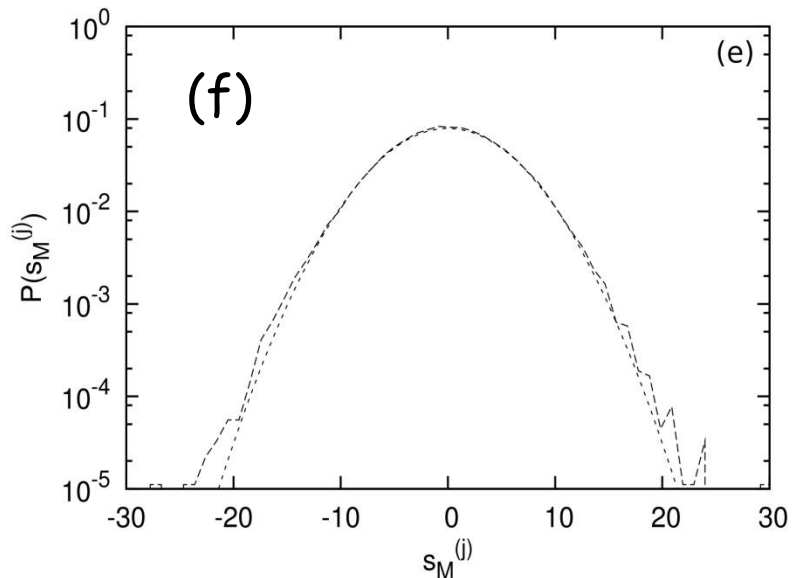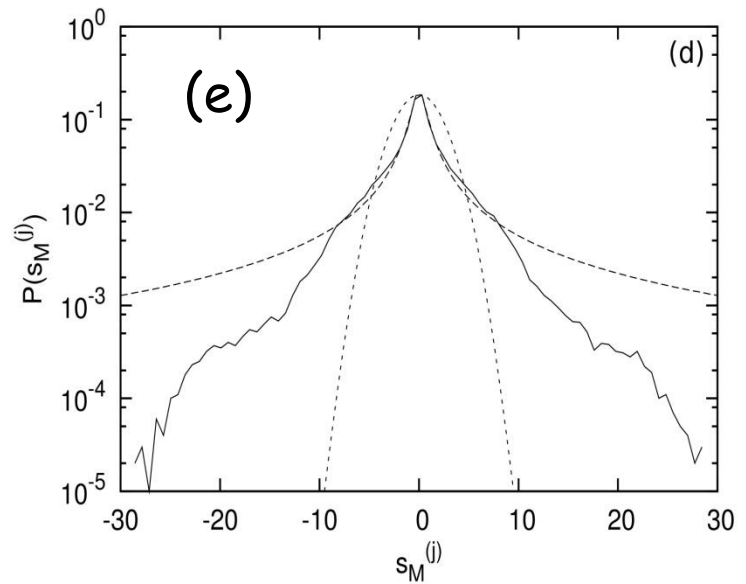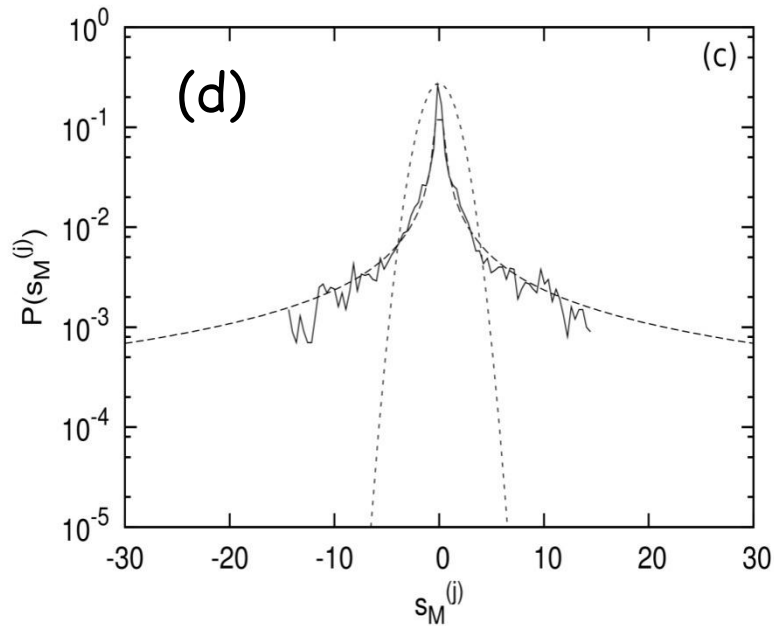
(a)
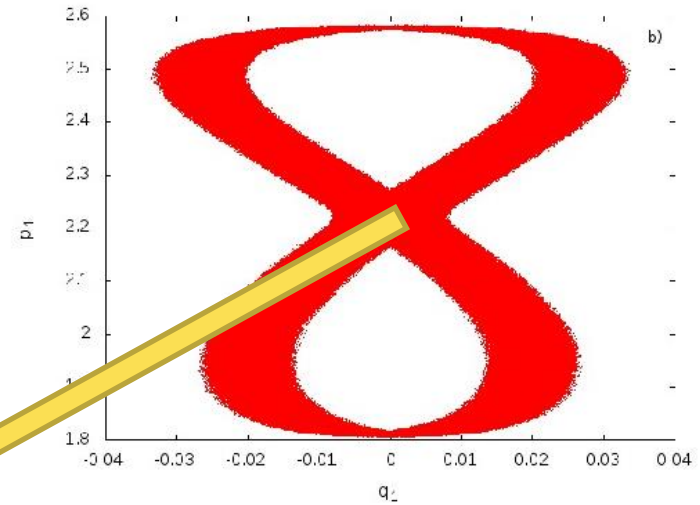
(b)

(c)

Figure 10: Orbits starting at a distance of $1.0*10^{-7}$ from the unstable SPO1 orbit, integrated for: **(a)** $t=10^5$ **(b)** $t=10^7$ **(c)** $t=10^8$ eventually escape in the large chaotic sea.

Figure 11(d – f) Plots of pdfs of position variables for a 5- particle FPU chain and initial conditions close to an unstable SPO1 orbit. The QSS observed here are well described by **q-Gaussians** with **(d) q = 2.78**, then **(e) q = 2.48**, until the orbit drifts away to a wide chaotic sea and the pdfs converge to **(f) Gaussians** with **q=1.05.**

5.2 Weak chaos in 2 – dimensional area – preserving maps

I have also studied chaotic orbits of a 2-dimensional area – preserving maps (modeling Hamiltonian systems of 2 – degrees of freedom) called the McMillan map

$$x_{n+1} = y_n$$

$$y_{n+1} = -x_n + \frac{2\mu y_n}{y_n^2 + 1} + \varepsilon y_n \qquad n = 0,1,2,3,.... \qquad (15)$$

near a saddle point at the origin ($\mu > 1$). Generally, the orbits wander around a chaotic domain and pass through a sequence of q-Gaussian states, with q > 1, until they become true Gaussians, with q = 1.

In some cases, however, when the chaotic domain extends around many islands where the orbits stick for long times, the pdfs appear to converge to a true q (>1)-Gaussian, for n $\rightarrow\infty$, as shown in Figure 14.
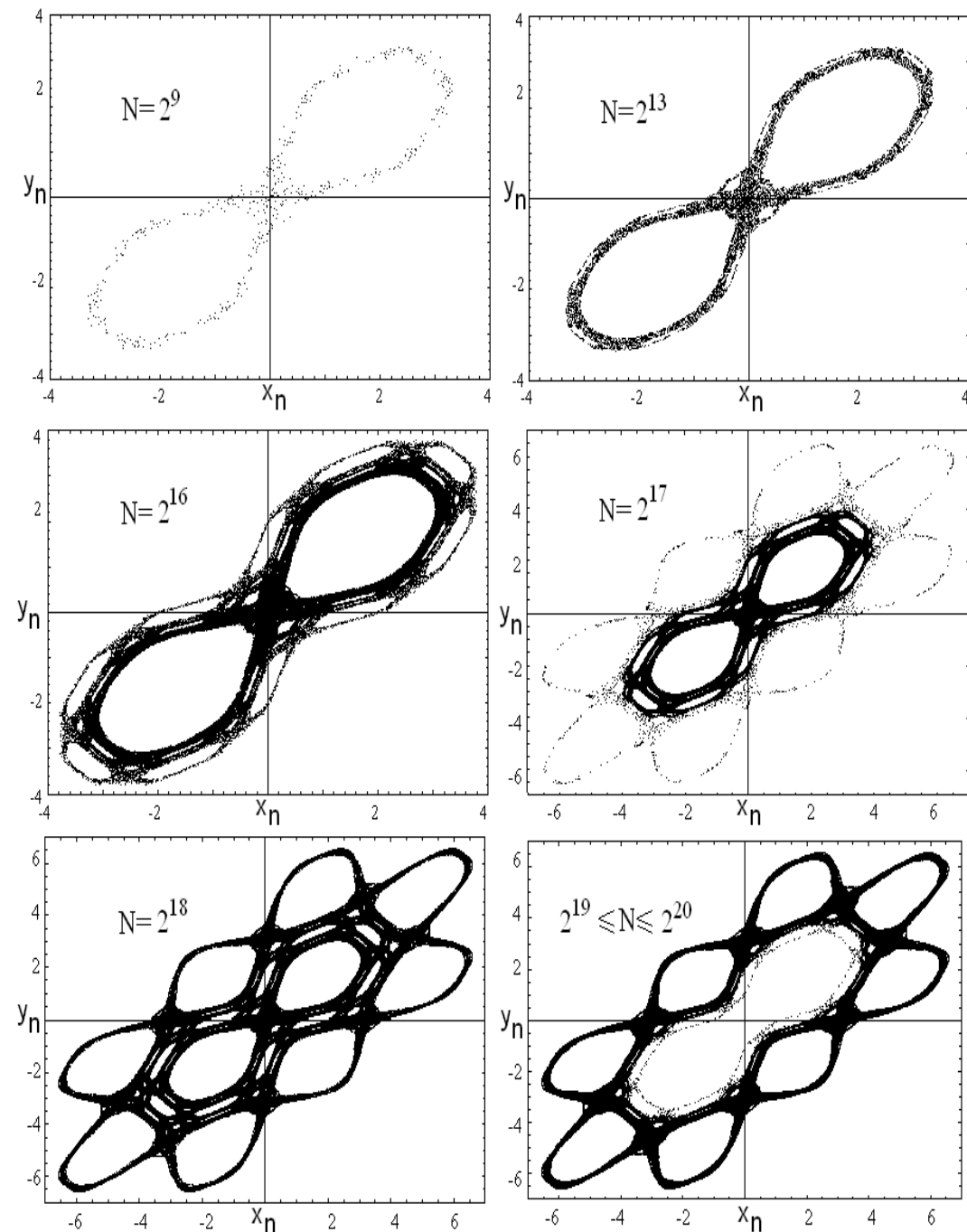
Figure 14 Left: Diffusive motion of orbits in a thin chaotic layer of a 2-d area – preserving map, starting near the unstable fixed point at the origin, evolving to N=2^{20} iterations. Below: The pdfs representing the normalized sum of the x_n coordinate of the map, converge to a q-Gaussian shown below, with q=1.6
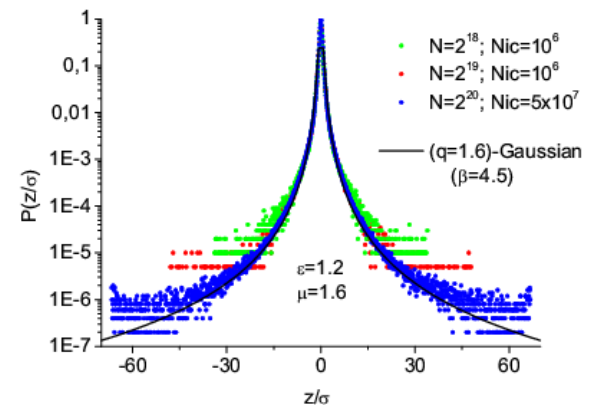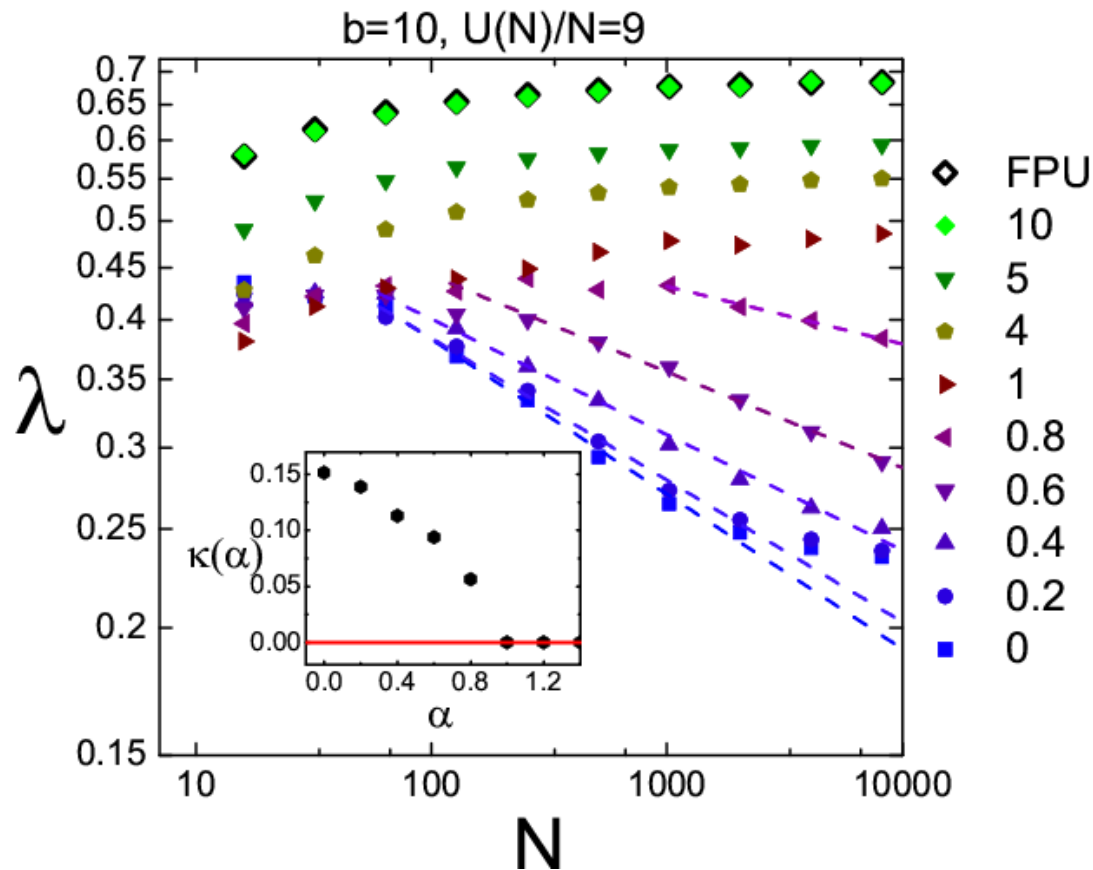
6. THE ROLE OF LONG RANGE INTERACTIONS

Let us now consider the case where our Hamiltonian involves Long Range Interactions (LRI) as follows:

$$H = \frac{1}{2}\sum_{n=1}^{N} p_n^2 + \frac{1}{2}\sum_{n=0}^{N}(x_{n+1} - x_n)^2 + \frac{b}{\tilde{N}(N,\alpha)}\sum_{n=0}^{N}\sum_{m=n+1}^{N}\frac{(x_n - x_m)^4}{//\,n-m\,//^{\alpha}} = U(N),$$

where b>0 and α ≥ 0. Note that to keep all energy terms in the Hamiltonian extensive, i.e. proportional to N, we have introduced before the quartic part of the potential the factor

$$\tilde{N}(N,\alpha) = \frac{1}{N}\sum_{i=0}^{N}\sum_{j=i+1}^{N}\frac{1}{(j-i)^{\alpha}} = \frac{1}{N}\sum_{i=0}^{N}\frac{N+1-i}{(i+1)^{\alpha}}$$

Figure 15: LRI restores order out of chaos! For 0 < α < 1 the maximal Lyapunov exponent λ starts to decay to zero as N increases and a "weaker" form of chaos is expected.

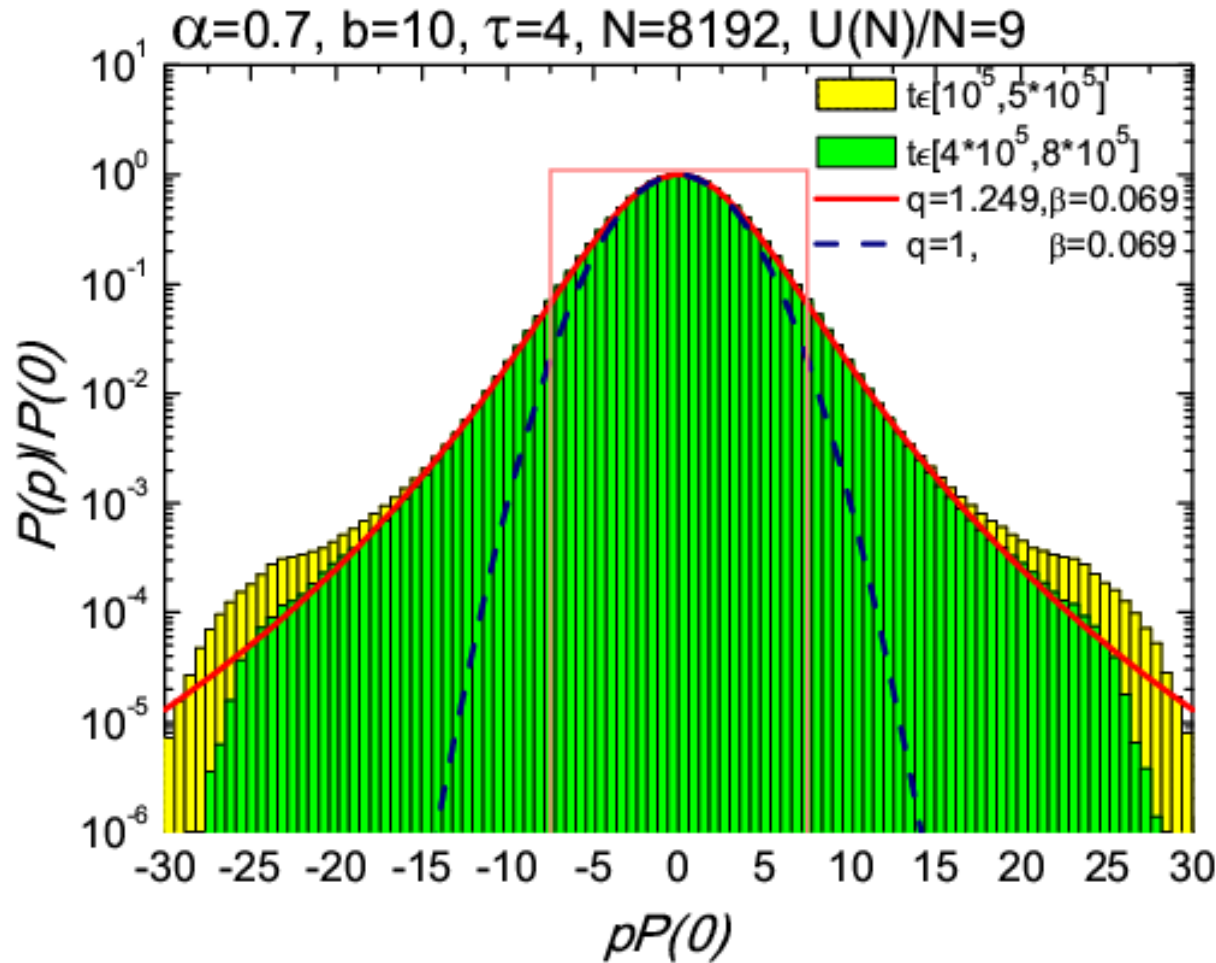**Figure 16:** The momentum probability density function (pdf) for Long Range Interactions, α = 0.7, converges to a q-Gaussian with q=1.249 indicating a "weaker" form of chaos as time increases.

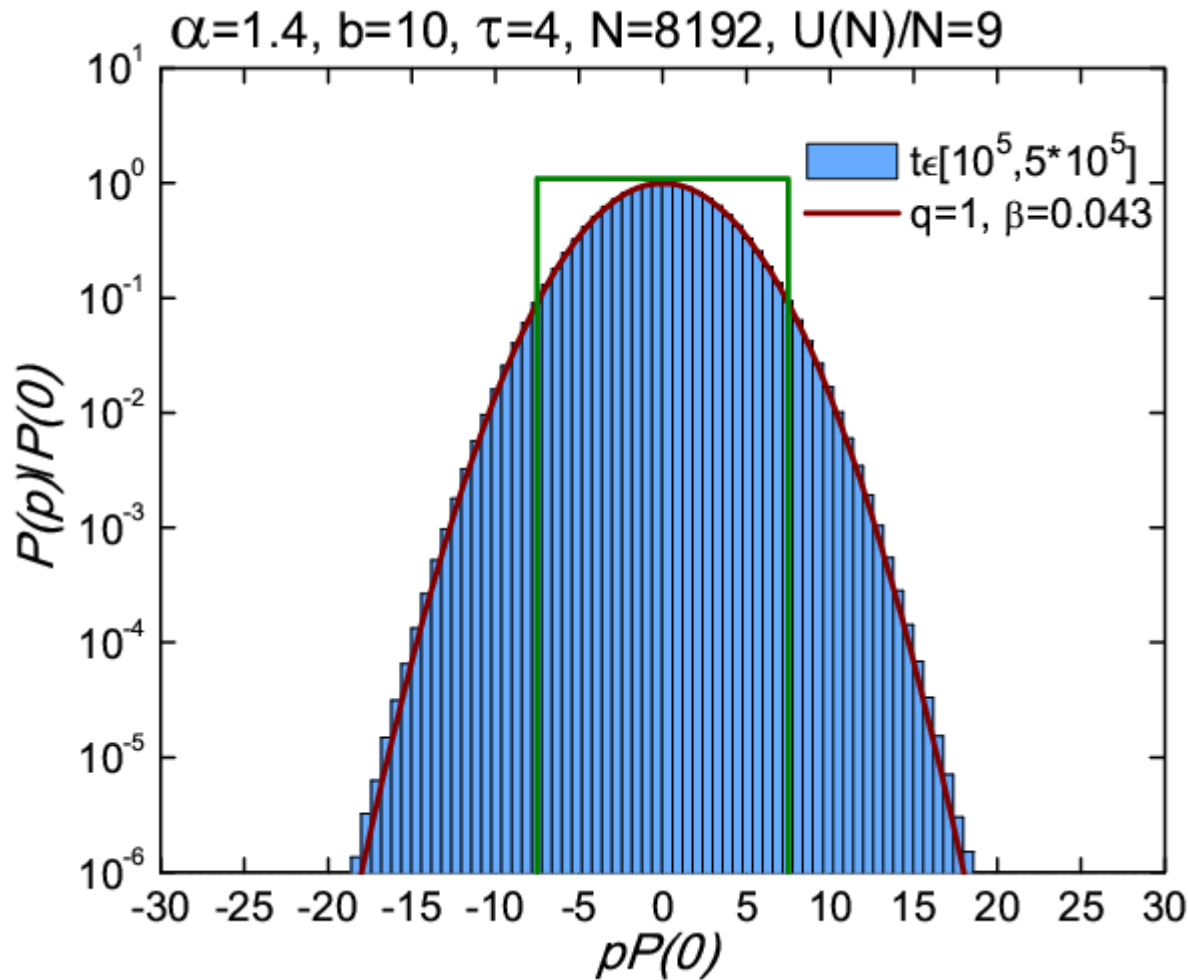**Figure 17:** On the contrary, the pdf of the momenta for Short Range Interactions, α = 1.4, quickly converges to a pure Gaussian, indicating "strong" chaos for α > 1.
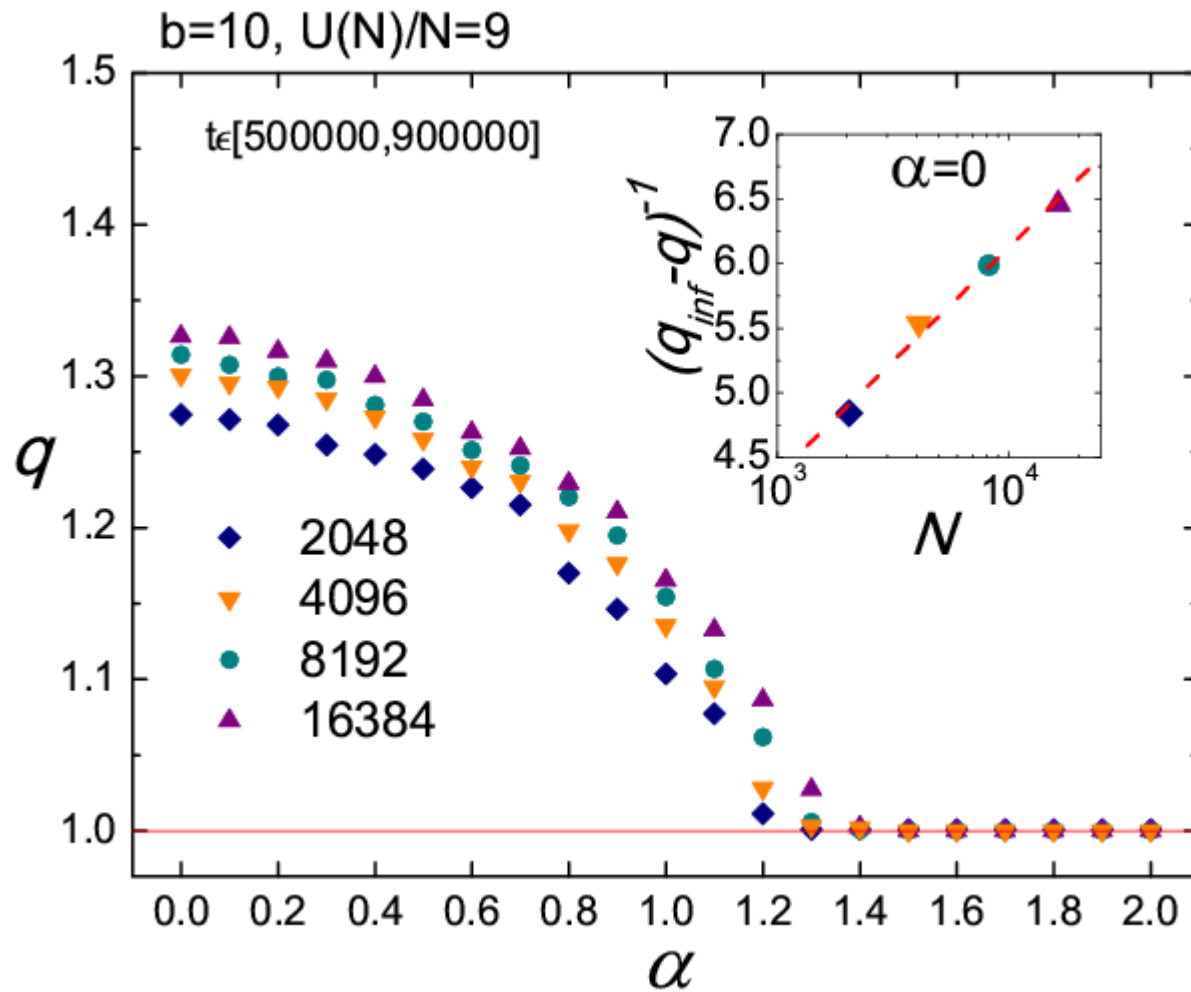
Figure 18: Note how the pdf index q decreases to 1 over the regime of Long Range Interactions, from α = 0 to just above α = 1, where Short Range Interactions take over.
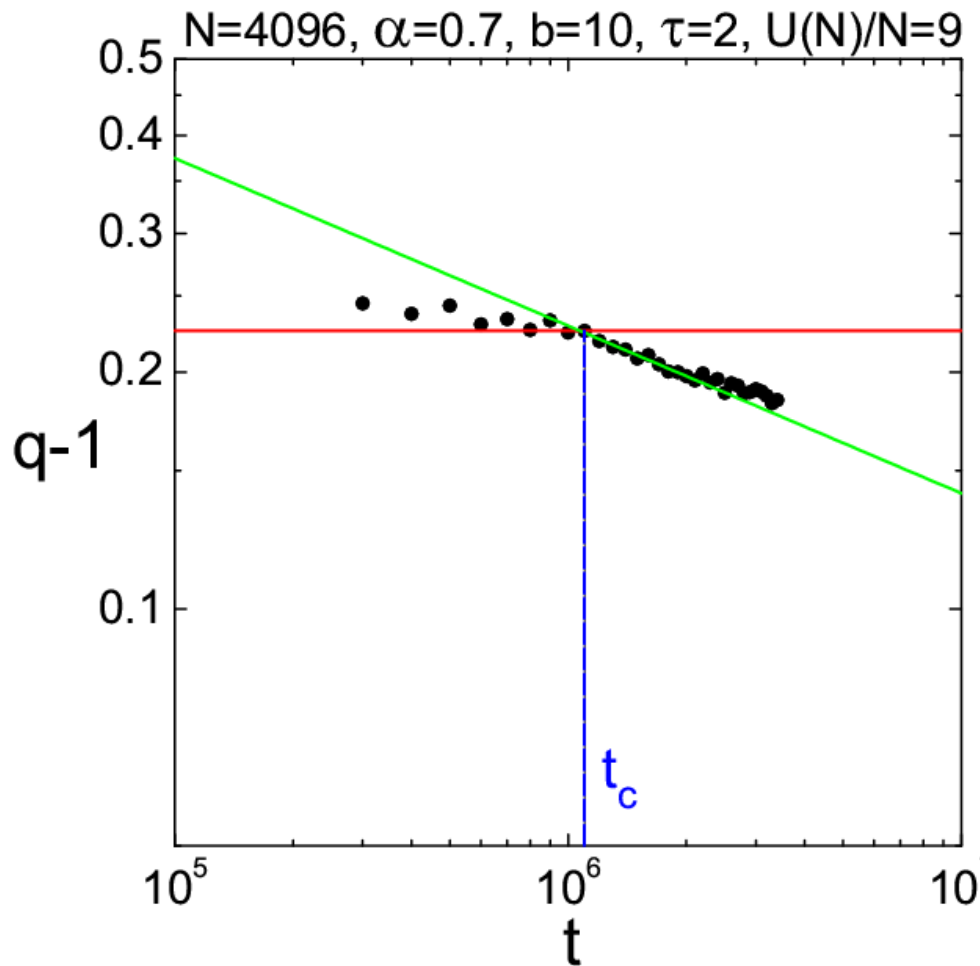
Figure 19a: Careful! Even for LRI, a= 0.7, the index q, starts to decrease towards 1 after a time threshold $t_c \approx 10^6$, for these parameter values.

Is that where Boltzmann and Gibbs are waiting for us?

Now fix the integration time: Note that the momentum pdfs tend to q- Gaussians as the number of particles grow!

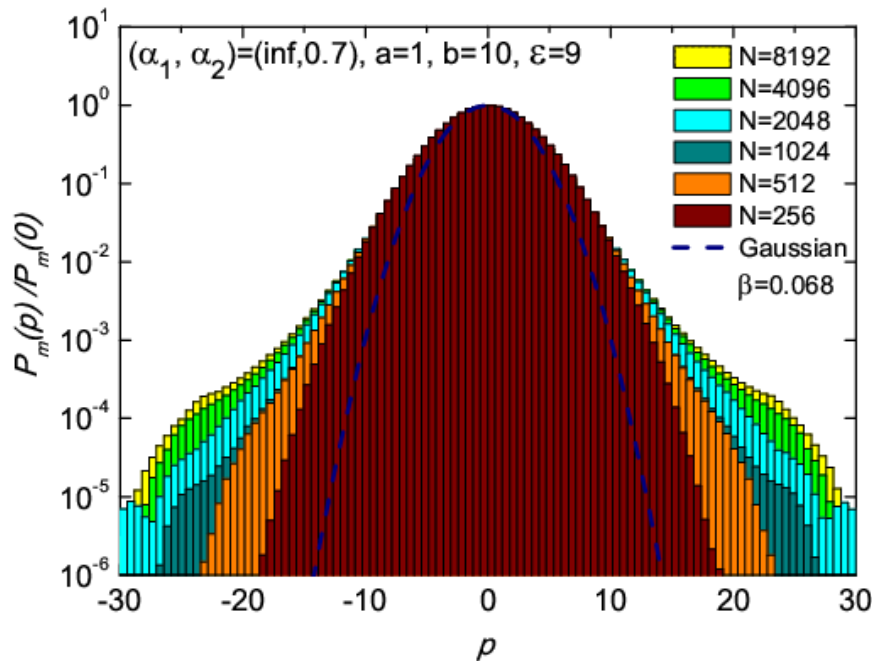

Figure 19b: Momentum distributions for the system with b = 10, ε = 9, α = 0.7 for increasing N values. Note that as N grows the pdfs are described by a q–Gaussian whose index q increases from 1.17 for N = 512 until 1.25 for N = 8192.

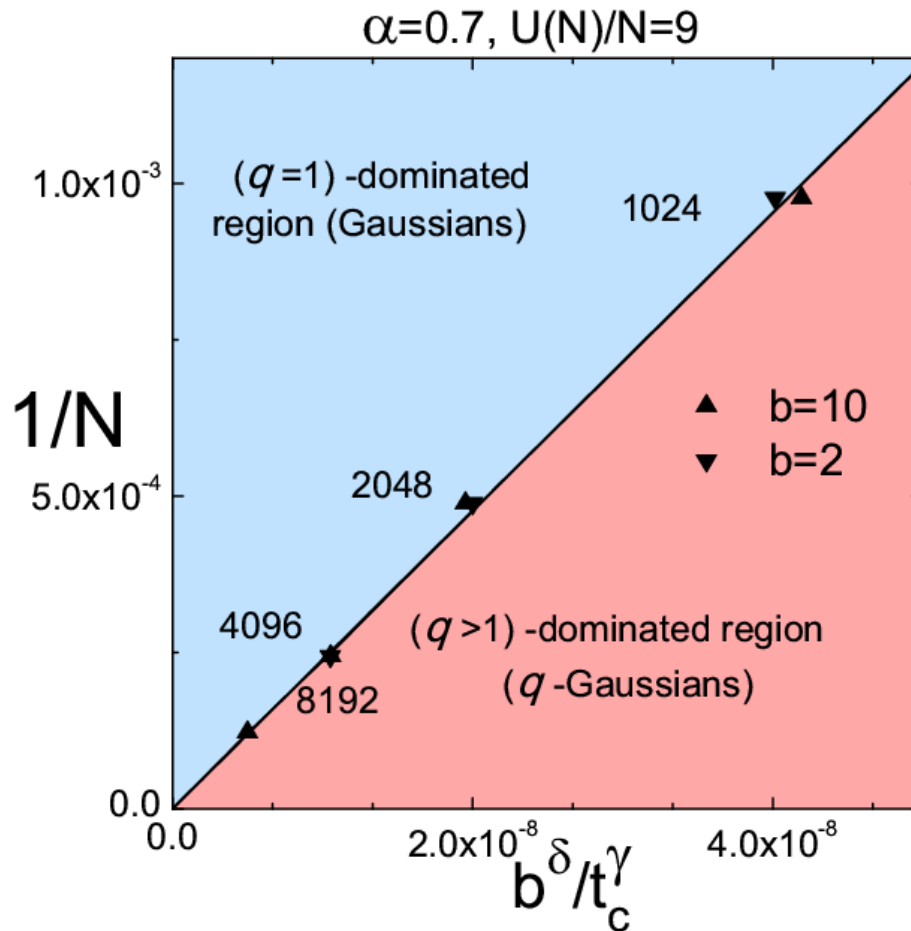**Figure 20:** **Very important**: A "phase transition diagram" is thus obtained, separating BG from Tsallis thermostatistics, in which the limits $t \to \infty$ and $N \to \infty$ do not commute!
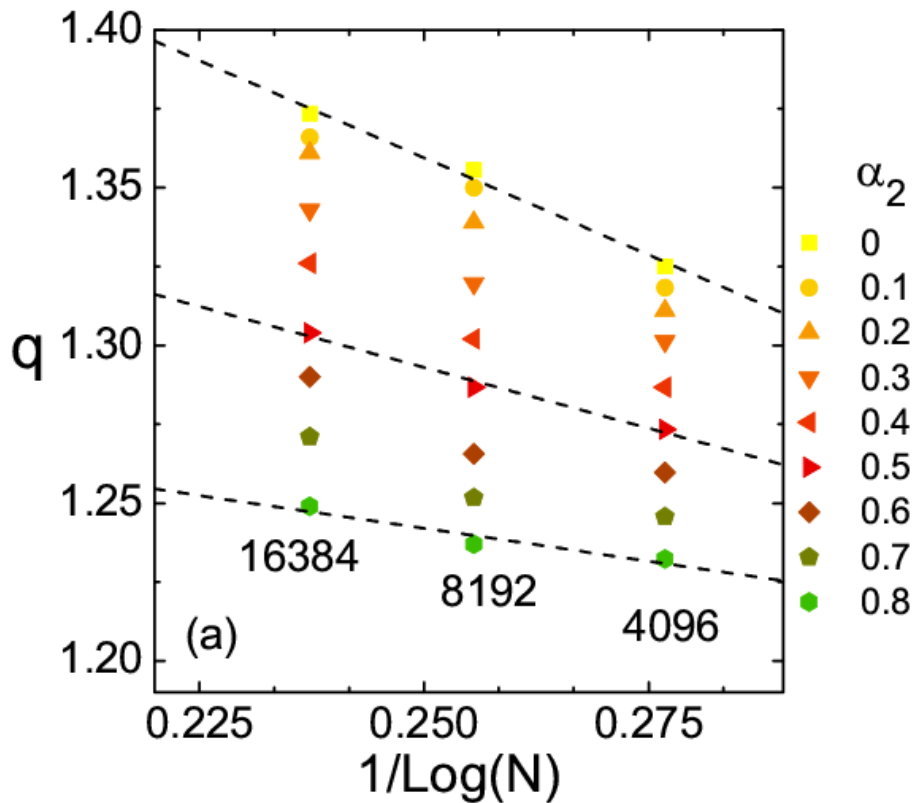
Figure 21: Important observation: The index q depends linearly on 1/ \log N for N=4096, 8192, 16384, as α changes, according the following formula:

$$q(N,\alpha) = q_\infty(\alpha) - \frac{c(\alpha)}{\log N}$$

Thus, we can use this formula to estimate the asymptotic behavior of q → q_∞ in the limit N → ∞!

Important Conclusion:
With LRI on the nonlinear forces, we find limiting values
$q_\infty > 1$ **as** $N \to \infty$ **, showing that the system remains**
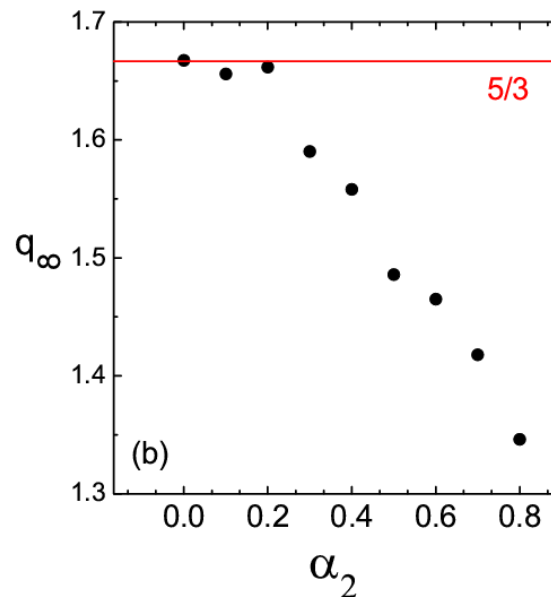**weakly chaotic in the thermodynamic limit!**

Figure 22: Variation of q_∞ **, as α changes. As** $α \to 1$ **, and beyond,**
one finds that $q_\infty \to 1$ **and we return to BG thermostatistics.**

6. CONCLUSIONS (What did we learn?)

Concerning Complex Dynamics of FPU 1-D Latiices:

1. We "described how important Nonlinear Normal Modes are in exploring "weak" and "strong" chaos, depending on the energy density $E_c/N > 0$ at which they first become unstable.

2. We mentioned the significance of Lyapunov spectra in quantifying strong chaos, and introduced the $GALI_k$ spectrum of indices $k=2,3,4,\ldots$, best suited for identifying chaos, when they vanish exponentially and quasiperiodic motion, when they decay as power laws, whose powers yield the dimensionality of the torus.

3. We used the GALI indices to study the breakdown of localization in 1-dimensional lattices: (i) In modal space connected to FPU recurrences and (ii) in position space, occurring in the form of discrete breathers.

Concerning Complex Statistics of FPU 1-D Lattices:

1. When Long Range Interactions are imposed (LRI) on the nonlinear forces (V_4) – for any range of linear interactions– we obtain weakly chaotic motion characterized by q-Gausian pdfs with q>1 (Tsallis thermodynamics).

2. In the LRI case, we find a "phase transition diagram", separating BG from Tsallis thermostatistics, in which the limits $t \to \infty$ and $N \to \infty$ do not commute!

3. When we introduce LRI only on the linear forces (V_2) we obtain strongly chaotic motion demonstrated by pure Gausian pdfs with q = 1 (Boltzmann Gibbs thermodynamics).

4. When LRI are imposed on the nonlinear forces, we find for long times limiting values $q_\infty > 1$ as $N \to \infty$, showing that the system remains weakly chaotic (Tsallis and NOT Boltzmann Gibbs) in the thermodynamic limit!

References

1. J. Bergamin, T. Bountis and C. Jung, "A Method for Locating Symmetric Homoclinic Orbits Using Symbolic Dynamics", J. Phys. A: Math. Gen., 33 , 8059-8070 (2000).

2. J. Bergamin, T. Bountis and M. Vrahatis, "Homoclinic Orbits of Invertible Maps", Nonlinearity 15, 1603 – 1619 (2002).

3. Skokos, Ch., Bountis, T., Antonopoulos, C. (2007), Geometrical properties of local dynamics in Hamiltonian systems: The generalized alignment index (GALI) method, Physica D231, 30—54.

4. Skokos, Ch., Bountis, T., Antonopoulos, C (2008), Detecting chaos, determining the dimensions of tori and predicting slow diffusion in Fermi Pasta-Ulam lattices by the generalized alignment index method. Eur. Phys. J. Sp. Top. 165, 5—14.

5. Christodoulidi, H., Efthymiopoulos, C., Bountis, T (2010), Energy localization on q-tori, long-term stability, and the interpretation of Fermi-Pasta-Ulam recurrences, Phys. Rev. E 81, 016210.

6. Antonopoulos, C., Bountis, T., Basios, V. (2011), Quasi-stationary chaotic states of multidimensional Hamiltonian systems, Physica A 390, 3290—3307.

7. Ruiz Lopez G., Bountis, T. and Tsallis, C. (2012), "Time – Evolving Statistics of Chaotic Orbits in Conservative Maps in the Context of the Central Limit Theorem", Intern. J. Bifurc. Chaos, Vol. 22 (9), pp. 12502.

8. Bountis T. and Skokos, H. (2012), *Complex Hamiltonian Dynamics*, Springer Synergetics series, Springer, Berlin.

9. Christodoulidi, H., Tsallis, C., Bountis, T. (2014), "Fermi-Pasta-Ulam model with long-range interactions: Dynamics and thermostatistics", EPJ Letters, 108, 40006 (2014) .

10. Christodoulidi, H. Bountis, T., Tsallis, C., Drossos, L., "Chaotic Behavior of the Fermi-Pasta-Ulam Model with Different Ranges of Particle interactions", J. Stat. Mech. 12 (12) (2016) 123206.

11. Christodoulidi, H., A. Bountis, A., Drossos, L., "The Effect of Long-Range Interactions on the Dynamics and Statistics of 1-D Hamiltonian Lattices with On-Site Potential", to appear in EPJST (2018).